Oceanographic conditions in the Atlantic zone in 2024

Peter S. Galbraith[1], Martine Lizotte[1], Marjolaine Blais[1], David Bélanger[2], Benoit Casault[3], Jonathan Coyne[2], Chantelle Layton[3], Kumiko Azetsu-Scott[3], Lindsay Beazley[3], Joël Chassé[4], Stephanie Clay[3], Frédéric Cyr[2,5], Emmanuel Devred[3], Alexandria Fudge[2], Carrie-Ellen Gabriel[3], Blair Greenan[3], Anne-Josée Hébert[1], Catherine L. Johnson[3], Gary Maillet[2], Jared Penney[2], Shannah Rastin[2], Marc Ringuette[3], Jean-Luc Shaw[1], Stephen Snook[2], Michel Starr[1]

[1]Fisheries and Oceans Canada, Québec Region, Maurice Lamontagne Institute, P.O. Box 1000, Mont-Joli, QC, G5H 3Z4

[2]Fisheries and Oceans Canada, Newfoundland and Labrador Region, Northwest Atlantic Fisheries Centre, P.O. Box 5667, St. John's NL A1C 5X1

[3]Fisheries and Oceans Canada, Maritimes Region, Bedford Institute of Oceanography P.O. Box 1006, 1 Challenger Drive Dartmouth, Nova Scotia, B2Y 4A2

[4]Fisheries and Oceans Canada, Gulf Region, Gulf Fisheries Centre, P.O. Box 5030, Moncton, NB E1C 9B6

[5]Center for Fisheries and Ecosystem Research, Fisheries and Marine Institute of Memorial University, St. John's, NL., A1C 5R3

2025

Canadian Technical Report of Hydrography and Ocean Sciences 400

Fisheries and Oceans Canada | Pêches et Océans Canada

Canada

Canadian Technical Report of Hydrography and Ocean Sciences

Technical reports contain scientific and technical information of a type that represents a contribution to existing knowledge but which is not normally found in the primary literature. The subject matter is generally related to programs and interests of the Oceans and Science sectors of Fisheries and Oceans Canada.

Technical reports may be cited as full publications. The correct citation appears above the abstract of each report. Each report is abstracted in the data base *Aquatic Sciences and Fisheries Abstracts.*

Technical reports are produced regionally but are numbered nationally. Requests for individual reports will be filled by the issuing establishment listed on the front cover and title page.

Regional and headquarters establishments of Ocean Science and Surveys ceased publication of their various report series as of December 1981. A complete listing of these publications and the last number issued under each title are published in the *Canadian Journal of Fisheries and Aquatic Sciences*, Volume 38: Index to Publications 1981. The current series began with Report Number 1 in January 1982.

Rapport technique canadien sur l'hydrographie et les sciences océaniques

Les rapports techniques contiennent des renseignements scientifiques et techniques qui constituent une contribution aux connaissances actuelles mais que l'on ne trouve pas normalement dans les revues scientifiques. Le sujet est généralement rattaché aux programmes et intérêts des secteurs des Océans et des Sciences de Pêches et Océans Canada.

Les rapports techniques peuvent être cités comme des publications à part entière. Le titre exact figure au-dessus du résumé de chaque rapport. Les rapports techniques sont résumés dans la base de données *Résumés des sciences aquatiques et halieutiques*.

Les rapports techniques sont produits à l'échelon régional, mais numérotés à l'échelon national. Les demandes de rapports seront satisfaites par l'établissement auteur dont le nom figure sur la couverture et la page de titre.

Les établissements de l’ancien secteur des Sciences et Levés océaniques dans les régions et à l'administration centrale ont cessé de publier leurs diverses séries de rapports en décembre 1981. Vous trouverez dans l'index des publications du volume 38 du *Journal canadien des sciences halieutiques et aquatiques*, la liste de ces publications ainsi que le dernier numéro paru dans chaque catégorie. La nouvelle série a commencé avec la publication du rapport numéro 1 en janvier 1982.

Canadian Technical Report
of Hydrography and Ocean Sciences 400

2025

Oceanographic conditions in the Atlantic zone in 2024

Peter S. Galbraith[1], Martine Lizotte[1], Marjolaine Blais[1],
David Bélanger[2], Benoit Casault[3], Jonathan Coyne[2], Chantelle Layton[3],
Kumiko Azetsu-Scott[3], Lindsay Beazley[3], Joël Chassé[4], Stephanie Clay[3], Frédéric Cyr[2,5],
Emmanuel Devred[3], Alexandria Fudge[2], Carrie-Ellen Gabriel[3], Blair Greenan[3],
Anne-Josée Hébert[1], Catherine L. Johnson[3], Gary Maillet[2], Jared Penney[2],
Shannah Rastin[2], Marc Ringuette[3], Jean-Luc Shaw[1], Stephen Snook[2], Michel Starr[1]

[1]Fisheries and Oceans Canada, Québec Region, Maurice Lamontagne Institute, P.O. Box 1000, Mont-Joli, QC, G5H 3Z4

[2]Fisheries and Oceans Canada, Newfoundland and Labrador Region, Northwest Atlantic Fisheries Centre, P.O. Box 5667, St. John's NL., A1C 5X1

[3]Fisheries and Oceans Canada, Maritimes Region, Bedford Institute of Oceanography P.O. Box 1006, 1 Challenger Drive Dartmouth, Nova Scotia, B2Y 4A2

[4]Fisheries and Oceans Canada, Gulf Region, Gulf Fisheries Centre, P.O. Box 5030, Moncton, NB, E1C 9B6

[5]Center for Fisheries and Ecosystem Research, Fisheries and Marine Institute of Memorial University, St. John's, NL., A1C 5R3

Cat. No. Fs97-18/400E-PDF ISBN 978-0-660-77877-8 ISSN 1488-5484

https://doi.org/10.60825/e92v-d229

Correct citation for this publication:

Galbraith, P.S., Lizotte, M., Blais, M., Bélanger, D., Casault, B., Coyne, J., Layton, C., Azetsu-Scott, K., Beazley, L., Chassé, J., Clay, S., Cyr, F., Devred, E., Fudge, A., Gabriel, C.-E., Greenan, B., Hébert, A.-J., Johnson, C.L., Maillet, G., Penney, J., Rastin, S., Ringuette, M., Shaw, J.-L., Snook, S., Starr, M. 2025. Oceanographic conditions in the Atlantic zone in 2024. Can. Tech. Rep. Hydrogr. Ocean. Sci. 400 : viii + 49 p. https://doi.org/10.60825/e92v-d229

This report is dedicated to the memory of Dr. Stéphane Plourde, a passionate research scientist who specialized in zooplankton studies. His knowledge significantly advanced our understanding of the Gulf of St. Lawrence ecosystem and contributed to better marine resource management. He was an important contributor to the Atlantic Zone Monitoring Program for over a decade and was a cherished collaborator and friend.

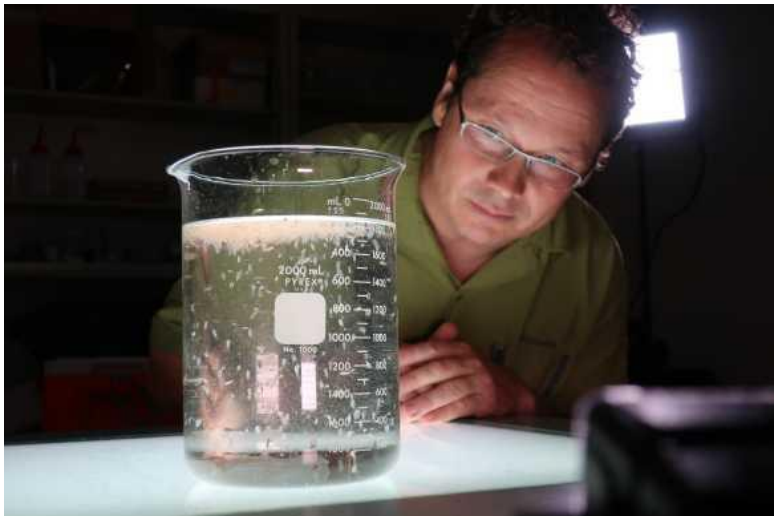

Photo credit: Karina Laberge

TABLE OF CONTENTS

Abstract vii
Résumé viii
1. Introduction 1
2. Physical Oceanographic Conditions 2
2.1 Annual Temperature Cycle 2
2.2 Sea Surface Temperature 2
2.1 The North Atlantic Oscillation 3
2.2 Cold Intermediate Layer 4
2.3 Sea ice 4
2.4 Labrador Current and Scotian Shelf Transport Index 5
2.5 Bottom and Deep Water Temperatures 5
2.6 Runoff and Stratification 6
2.7 Conditions at AZMP High Frequency Sampling Stations 6
2.8 Summary 6
3. Biogeochemical Environment 7
3.1 Nutrients 8
3.2 Phytoplankton 9
3.3 Zooplankton 10
4. Chemical Oceanographic Conditions 11
4.1 Dissolved oxygen saturation 12
4.2 CO_2-Carbonate system 13
4.2.1 Inorganic carbon state variables 13
4.2.2 Potential of hydrogen (pH) 14
4.2.3 Partial pressure of CO_2 15
4.2.4 Calcium carbonate saturation states and substrate-inhibitor ratio 15
5. Conclusion 17
5.1 Summary 18
Acknowledgments 22
References 23

ABSTRACT

Galbraith, P.S., Lizotte, M., Blais, M., Bélanger, D., Casault, B., Coyne, J., Layton, C., Azetsu-Scott, K., Beazley, L., Chassé, J., Clay, S., Cyr, F., Devred, E., Fudge, A., Gabriel, C.-E., Greenan, B., Hébert, A.-J., Johnson, C.L., Maillet, G., Penney, J., Rastin, S., Ringuette, M., Shaw, J.-L., Snook, S., Starr, M. 2025. Oceanographic conditions in the Atlantic zone in 2024. Can. Tech. Rep. Hydrogr. Ocean. Sci. 400 : viii + 49 p. https://doi.org/10.60825/e92v-d229

This summarizes oceanographic conditions for 2024 detailed in Atlantic Zone Monitoring Program (AZMP) reports. Sea surface temperatures were overall second highest since 1982. Sea ice was at a record low in the Gulf of St. Lawrence. Since around 2010, deep water temperatures and dissolved oxygen on the Scotian Shelf and Gulf of St. Lawrence had been greatly influenced by an increasing proportion of warm saline waters relative to cold fresh Labrador Water in recent years, but this peaked in 2022. In recent years, most regions exhibited either lower-than-normal nitrate levels in the subsurface layer, later-than-normal fall bloom onset, and/or higher-than-normal phytoplankton biomass accumulation during fall. *Calanus finmarchicus* returned to above-normal abundances in most regions in the past two years. Several metrics of ocean acidification have exhibited overall trends of deterioration. Near-bottom water pH levels, aragonite and calcite saturation states were below normal across most regions. Aragonite saturation was below the dissolution threshold (Ω_A <1) in the Gulf of St. Lawrence and at Station 27. The most critical chemical conditions are observed in near-bottom waters of the St. Lawrence Estuary and northwest Gulf, where both hypoxic conditions (oxygen saturation <30%) and hypercapnic conditions (pCO_2 >1,000 µatm) persist.

RÉSUMÉ

Galbraith, P.S., Lizotte, M., Blais, M., Bélanger, D., Casault, B., Coyne, J., Layton, C., Azetsu-Scott, K., Beazley, L., Chassé, J., Clay, S., Cyr, F., Devred, E., Fudge, A., Gabriel, C.-E., Greenan, B., Hébert, A.-J., Johnson, C.L., Maillet, G., Penney, J., Rastin, S., Ringuette, M., Shaw, J.-L., Snook, S., Starr, M. 2025. Oceanographic conditions in the Atlantic zone in 2024. Can. Tech. Rep. Hydrogr. Ocean. Sci. 400 : viii + 49 p. https://doi.org/10.60825/e92v-d229

Ceci résume les conditions océanographiques 2024 détaillées dans les rapports du Programme de monitorage de la zone atlantique (PMZA). Les températures de surface moyenne étaient les secondes plus élevées. La glace de mer était à un niveau historiquement bas dans le golfe. Depuis environ 2010, les températures des eaux profondes et l'oxygène dissous sur le plateau néo-écossais et dans le golfe ont été grandement influencés par une proportion croissante d'eaux salées chaudes par rapport aux eaux froides du Labrador, mais cette tendance a culminé en 2022. La plupart des régions ont affiché de faibles inventaires de nitrate dans la couche de subsurface, un début de floraison automnale tardif et/ou une forte biomasse phytoplanctonique pendant l'automne. *Calanus finmarchicus* est revenu à des abondances supérieures à la normale dans la plupart des régions. Plusieurs indicateurs d'acidification révèlent une détérioration générale. Le pH des eaux près du fond et les états de saturation en aragonite et en calcite étaient faibles dans la plupart des régions. La saturation en aragonite était inférieure au seuil de dissolution (Ω_A <1) dans le golfe et à la station 27. Les conditions chimiques les plus critiques sont observées dans les eaux profondes de l'estuaire et du nord-ouest du golfe, où persistent des conditions hypoxiques (saturation en oxygène <30%) et hypercapniques (pCO_2 >1,000 µatm).

1. INTRODUCTION

The Atlantic Zonal Monitoring Program (AZMP) was implemented in 1998 (Therriault et al. 1998) with the aim of:

1. Increasing Fisheries and Oceans Canada's (DFO's) capacity to understand, describe, and forecast the state of the marine ecosystem; and
2. Quantifying the changes in ocean physical, chemical, and biological properties.

A critical element of the AZMP is an annual assessment of the physical, biological and chemical oceanographic conditions.

A description of the distribution in time and space of temperature, salinity, nutrients (nitrate, silicate, phosphate), gases dissolved in seawater (oxygen, carbon dioxide (CO_2)), and plankton provides important information on water-mass movements, on the locations, timing, and magnitude of biological production cycles, and ocean chemistry parameters. Understanding the production cycles of plankton, alongside changing physical and chemical conditions, is crucial for an ecosystem-based approach to stock assessment, marine protection and conservation, as well as fisheries and species at risk management.

The AZMP derives its information on the state of the marine ecosystem from data collected at a network of locations (high-frequency sampling stations, cross-shelf sections and ecosystem surveys) in each of DFO's administrative regions of Eastern Canada (Quebec, Maritimes, Gulf, Newfoundland and Labrador) sampled at frequencies ranging from weekly to annually (Figure 1). This annual assessment has included Labrador Sea observations collected by the Atlantic Zone Off-Shelf Monitoring Program (AZOMP) since the report on 2015 conditions. Information on ocean acidification was first presented in the report on 2018 conditions.

The sampling design provides information on the variability in physical, chemical, and biological properties of the northwest Atlantic continental shelf. Multispecies trawl surveys and cross-shelf sections provide detailed geographic information but are limited in their seasonal coverage. Strategically placed high-frequency sampling stations complement the broad scale sampling by providing more detailed information at a greater temporal resolution. Sampling procedures are standardized across the zone and described in Mitchell et al. (2002). In addition, glider missions annually sample about 15,000 profiles of temperature, salinity, oxygen, optical backscatter, chlorophyll and CDOM fluorescence, mostly on the Halifax Line. Real time oceanographic buoys collected over 1500 vertical profiles throughout the zone in 2024.

Environmental conditions are usually expressed as anomalies, i.e., deviations from their long-term mean. The long-term mean or normal conditions are calculated, when possible, for the 1991–2020 reference period for physical parameters, 1999–2020 for biological parameters and 2014–2020 for CO_2-carbonate system parameters and oxygen saturation. Furthermore, because these variables have different units (°C, km^3, km^2, etc.) and ranges of variability, each anomaly time series is normalized by dividing by its standard deviation (SD), which is calculated using annual averages from the reference period. This allows direct comparison of the various series. Missing data are represented by grey cells, and near-normal conditions by white cells. Conditions within ± ½ SD of the average are considered to be near normal for physical and CO_2-carbonate parameters while a second threshold of ± ⅓SD is used for biological parameters to enhance the detection of biological patterns, considering their significant interannual variability. Conditions with higher than normal values are shown as red cells. However, for quantities that decrease with warmer temperatures (e.g., ice volumes and cold water volumes or

areas), red indicates reduced levels, with more intense reds representing greater reductions. Conversely, blue represents lower than normal values, except for increased sea ice and cold water areas and volumes. Higher than normal freshwater inflow, salinity or stratification are shown as red, but do not necessarily correspond to warmer than normal conditions. While we often describe the environment in terms of anomalies relative to the climatological period, it remains important to look at the long-term trends. We also often speak in terms of rank and series records which help to paint a broader picture.

2. PHYSICAL OCEANOGRAPHIC CONDITIONS

Peter S. Galbraith, Jonathan Coyne, Chantelle Layton, Frédéric Cyr, Joël Chassé, Blair Greenan, Jean-Luc Shaw, Jared Penney.

This is a summary of physical oceanographic conditions during 2024 for eastern Canadian oceanic waters (Figures 1 and 2) as reported annually by the AZMP in technical reports (e.g., Galbraith et al. 2024a, Cyr et al. 2024 and Hebert et al. 2024 for conditions in 2023). Unless otherwise noted, the methodologies documented in these past reports are used here. Detailed descriptions of conditions in 2024 will be published in similar reports.

2.1 ANNUAL TEMPERATURE CYCLE

Ocean temperature varies vertically through the seasons in the Atlantic Zone (Figure 3). The summertime temperature (T) structure consists of three distinct layers: the summertime warm surface layer, the cold intermediate layer (CIL), and the deeper water layer. During fall and winter, the surface layer deepens and cools mostly from wind-driven mixing and heat loss to the atmosphere prior to ice formation, but also partly because of reduced runoff and brine rejection associated with sea ice formation where it occurs. The surface winter layer extends to an average depth of about 50 m on the Scotian Shelf, 75 m in the Gulf of St. Lawrence by March, and can extend to the bottom (>150 m) on the Labrador and Newfoundland Shelves. It reaches near-freezing temperatures in the latter two areas. During spring, surface warming, sea ice melt waters, and continental runoff lead to a lower salinity and higher temperature surface layer, below which cold waters from the previous winter are partly isolated from the atmosphere and form the summer CIL. This layer persists until the next winter, gradually warming and deepening during summer (Gilbert and Pettigrew 1997, Cyr et al. 2011). The CIL is, for the most part, locally formed in winter in separate areas around the zone (Galbraith 2006, Umoh and Thompson 1994, Umoh et al. 1995). For example, the temperature minimum of the winter mixed layer occurs at about the same time in March both on the Scotian Shelf and in the Gulf of St. Lawrence, reaching different minimum temperatures; an indication of local formation rather than advection from one region to the other. However, transport occurs later in the year from the Labrador Shelf to the Gulf of St. Lawrence (Galbraith 2006) and Newfoundland Shelf (Umoh et al. 1995) and from the Gulf of St. Lawrence to the St. Lawrence Estuary (Galbraith 2006) and the Scotian Shelf (Umoh and Thompson 1994). The temperature minimum in southern parts of the Newfoundland Shelf (e.g., at Station 27) can occur well after winter; for example, in 2021 it was observed in June-July. Deep waters are defined here as those below the CIL that have only weak seasonal cycles.

2.2 SEA SURFACE TEMPERATURE

The satellite-based sea surface temperature (SST) product is again revised this year. It blends data from Pathfinder version 5.3 (4 km resolution for 1982–1985 and sparsely to 2020; Casey et al. 2010), Maurice Lamontagne Institute (MLI; 1.1 km resolution for 1985–2000 and sparsely to 2013; Larouche & Galbraith 2016) with the NOAA STAR CoastWatch Advanced Clear-Sky

Processor for Ocean (ACSPO) L3S-LEO-Daily “super-collated” v2.81 product (0.02 degree resolution for 2000 to current; Jonasson et al. 2022). Details of the regional calibration are found in Galbraith et al. 2025. Certain previously reported records have changed because the SST blend is different than in previous reports, although the overall patterns remain the same. The main difference is that the new product ranks 2012 as the warmest year on record whereas it was 4th in the previously used product. The better coverage of the new product as well as comparisons to *in-situ* observations give confidence that this is correct.

Monthly temperature composites are calculated from averaged daily anomalies to which monthly climatological average temperatures are added (Galbraith et al. 2021). Figures 4 and 5 show monthly temperature composites and anomalies, and Figures 6 and 7 show area-averaged values by month and for the ice-free season over the averaging areas shown in Figure 2 (top panel). New in this report is the addition of NAFO 5Y and 5Ze covering the Gulf of Maine.

Averaged over ice-free periods of the year as short as June to November on the Labrador Shelf, May to November in the Gulf, to the entire year on the Scotian Shelf, air temperature has been found to be a good proxy of sea surface temperature. Therefore, the warming trend observed in air temperature since the 1870s of about 1 °C per century is also expected to have occurred in surface water temperatures across Atlantic Canada (Galbraith and Larouche 2013, Galbraith et al. 2021).

In 2024, monthly average sea surface temperatures were generally normal to above normal during ice-free periods, with larger anomalies in the north than in the south (Figure 6). Of the 171 reported regional monthly averages, a total of 133 were above normal, including 20 series records. Only 6 were below normal, 4 of them occurring in December. Sea surface temperature seasonal averages were above normal across the zone (Figure 7), reaching record highs in parts of the Newfoundland Shelf (3K, 3L, 3N), over the entire Gulf of St. Lawrence and east of Cape Breton (4Vn).The spatially weighted zonal average was second highest of the time series, with 2012 ranking first. The last four years ranked 2nd to 5th warmest after the record of 2012. The addition of NAFO 5 Gulf of Maine areas to the weighted zonal average decreased the value of the 2024 SST index (from 2.0 to 1.8) compared to the zonal average that would have been computed without these areas, as in previous reports.

2.1 THE NORTH ATLANTIC OSCILLATION

The North Atlantic Oscillation (NAO) index (Figure 7) is based on the sea-level atmospheric pressure difference between the sub-equatorial high and subpolar low and quantifies the dominant winter atmospheric forcing over the North Atlantic Ocean. Two versions of the winter NAO are used here. The first is the December-March average of the monthly time series from the National Oceanic and Atmospheric Administration (NOAA). The second is the Hurrell principal-component based index from the National Center for Atmospheric Research (NCAR). Both indices are similar in most years, but in some years, they differ markedly because of unusual pressure patterns. This has been the case more often in recent years, including in 2024.

The atmospheric patterns described by the NAO affect winds, air temperature, precipitation, and hydrographic properties on the eastern Canadian seaboard either directly or through advection. Strong northwest winds, cold air and sea temperatures, and heavy ice in the Labrador Sea area have usually been associated with a high positive NAO index, with opposite effects occurring with a negative NAO index. The minimum value on record of the NOAA index was reached in 2010, coinciding with warmer than normal conditions. The recent positive streak (normally indicative of colder conditions) has, however, not coincided with winter conditions as cold as in

the previous positive streak of the late-1980's/early-1990s. In 2024, the winter NOAA NAO index was positive (cold) at +0.8 while the Hurrell NAO index was near normal.

2.2 COLD INTERMEDIATE LAYER

For the Newfoundland and Labrador Shelf, the CIL indices shown in Figure 7 are the cross-sectional areas of waters with T <0 °C during summer along the Seal Island, White Bay, Bonavista and Flemish Cap AZMP sections (Cyr et al. 2024). For the Gulf, the CIL volume with T <1 °C observed in August-September (excluding the Mécatina Trough) is used (Galbraith et al. 2024a). Because the CIL reaches to the bottom on the Magdalen Shallows in the Southern Gulf, the area of the bottom occupied by waters colder than 1 °C during the September survey is also used as a CIL index specific to that area (Galbraith et al. 2024a). For the Scotian Shelf, the volume with T <4 °C observed in July is used (Hebert et al. 2023). The CIL indices reported here are taken at about the same time within their respective annual cycles, although not simultaneously.

The Gulf of St. Lawrence CIL volume was at record low in 2021, representing record-warm conditions. The volume in summer 2024, while over twice as large as 2021, was fifth lowest. The CIL volume on the Scotian Shelf was at a record low in 2022, increased to near normal in 2023 and was again near normal in 2024. The CIL areas at the four AZMP sections on the Newfoundland and Labrador shelf were all below normal after some near-normal conditions in 2023.

2.3 SEA ICE

Because the CIL and sea ice cover are both formed in winter, it is not surprising that indices for both are well correlated with each other and with winter air temperature and show the North-South advective nature of properties on the Newfoundland and Labrador Shelf. Seasonal average sea ice volume on the Southern Labrador Shelf is correlated with the CIL area further south along the Bonavista section (1980–2020, $R^2 = 0.70$) whereas Newfoundland Shelf sea ice metrics are correlated with December-March air temperature further north at Cartwright (1969–2023, $R^2 = 0.62–0.78$; Cyr et al. 2024). In the Gulf of St. Lawrence, the correlation between the December-March air temperature averaged over multiple coastal meteorological stations and the maximum annual ice volume reaches $R^2 = 0.76$ (1969–2024; Galbraith et al. 2024b). Air temperature is similarly well correlated to sea ice cover area and duration ($R^2 = 0.82–0.84$, 1969–2024; Galbraith et al. 2024b). Sensitivity of the Gulf of St. Lawrence ice cover to climate change can be therefore estimated using past patterns of change in winter air temperature and sea ice features, which indicate losses of 18 km^3, 32,000 km^2 and 14 days of sea ice season for each 1 °C increase in winter air temperature (Galbraith et al. 2024b).

Sea ice conditions on the Newfoundland and Labrador Shelf are provided by an index that encompasses duration and seasonal maximum area in three regions: Northern Labrador Shelf, Southern Labrador Shelf and Newfoundland Shelf (Cyr and Galbraith 2021). The index was second lowest in 2010, reached a record low in 2011, rebounded during 2014–2016 when heavy sea ice conditions were observed (Figure 7). It has been near or below normal since, including 3rd lowest in 2021 and below normal (-1.0 SD) in 2024.

Sea ice conditions in the Gulf of St. Lawrence and the Scotian Shelf have been below normal since 2010 except for a rebound in 2014 and 2015. The period includes four nearly ice-free winters (Galbraith et al. 2024b). In the fifteen-year period between 2010 and 2024, the seasonal average sea ice volume had eleven of the fifteen lowest values of the 56-year time series. Record lows were reached in 2024 for both the seasonal weekly maximum (not shown) and the seasonal average volume (January to April; Figure 7). The 2024 sea ice season experienced 44

days of ice volumes below historical records for those days. No ice was exported onto the Scotian Shelf.

2.4 LABRADOR CURRENT AND SCOTIAN SHELF TRANSPORT INDEX

The annual-mean Labrador Current transport index (Han et al. 2014, Cyr et al. 2024) shows that transport along the Newfoundland and Labrador shelf break is sometimes out of phase with transport on the Scotian shelf break (Figure 7). Transport was strongest in the early 1990s and weakest in the mid-2000s over the Newfoundland and Labrador Shelf break, and opposite over the Scotian Shelf break. While there is a negative correlation between these two indices, the relationship is not statistically significant. Both transport indices are respectively positively (R^2= 0.20, p=0.009) and negatively (R^2= 0.13, p=0.039) correlated with a winter NAO index lagged by one year. Variations in the westward transport of Labrador Slope Water from the Newfoundland region along the shelf break have been shown to have a strong effect on water masses of the Scotian Shelf deep basins, with increased transport through Flemish Pass associated with below normal deep temperatures and salinities on the Scotian Shelf and in the Gulf of Maine. The transport was near normal along the Newfoundland and Labrador Shelf break but at a record high along the Scotian Shelf break, above normal for the second consecutive year. This indicates increased input of cold and low salinity waters with high dissolved oxygen concentrations that may feed into the Gulf of St. Lawrence and Scotian Shelf at depth.

2.5 BOTTOM AND DEEP WATER TEMPERATURES

Interdecadal changes in temperature, salinity, and dissolved oxygen of the deep waters of the Gulf of St. Lawrence, Scotian Shelf, and Gulf of Maine are related to the varying proportion of their source waters: cold, fresh, high-dissolved-oxygen Labrador Current water and warm, salty, low-dissolved oxygen Warm Slope Water, also called North Atlantic Central Waters (Gilbert et al. 2005, Jutras et al. 2020). The mixing ratio may be controlled by the retroreflection of the Labrador Current at the tip of the Grand Banks (Jutras et al. 2023a). The >150 m water layer of the Gulf of St. Lawrence below the CIL originates from an inflow at the entrance of the Laurentian Channel which circulates towards the heads of the Laurentian, Anticosti, and Esquiman Channels in up to roughly three to nearly five years at 300 m after reaching Cabot Strait, with limited exchange with shallower upper layers (Gilbert et al. 2004, Stevens et al. 2024, Rousseau et al. 2025). The mixing ratio of waters entering the Laurentian Channel was reported to have reached 100% of the warm component in 2021 (Jutras et al. 2023b). Deeper portions of the Scotian Shelf and Gulf of Maine are similarly connected to the slope through deep channels that cut into the shelves from the shelf break. Deep basins such as Emerald Basin undergo very large interannual and interdecadal variability of the bottom water temperature associated with deep renewal events. More regular changes associated with circulation are observed in bottom water temperature over the central and eastern Scotian Shelf (NAFO Divisions 4W and 4Vs respectively). Bathymetry in these areas is fairly evenly distributed between 30 m and 170 m, with 4Vs including some 400–450 m depths from the Laurentian Channel. Both these areas are therefore affected somewhat by CIL waters as well as the waters underneath.

In 2024, bottom temperatures in areas affected by the CIL were above normal in all regions of the Newfoundland and Labrador Shelf and Gulf of St. Lawrence (Figure 7). Bottom temperatures in the deep channels of the Gulf of St. Lawrence and the Scotian Shelf, which are affected by the mixture of cold, fresh and warm, saline waters, show decreases from the 2022 record highs. In the Gulf of St. Lawrence, temperatures decreased to values similar to those of 2020. On the Scotian Shelf, they have decreased to near normal in regions 4V and 4X and even to below normal for the first time since 2008 in region 4W.

2.6 RUNOFF AND STRATIFICATION

Freshwater runoff in the Gulf of St. Lawrence, particularly within the St. Lawrence Estuary, strongly influences circulation, salinity, and stratification (and hence upper-layer temperatures) in the Gulf and, via the Nova Scotia Current, on the Scotian Shelf. The runoff product is based on daily runoff estimated at Quebec City that is then lagged by 3 weeks to account for transport time to the Estuary, then combined with output from a hydrological watershed model for rivers flowing into the Estuary to form the RIVSUM II (Galbraith et al. 2024a). The inter-annual variability of seasonal (May—October) stratification (0–50 m) at Rimouski Station in the Estuary is correlated with seasonally averaged RIVSUM II runoff (1991–2024; $R^2 = 0.65$, Figure 8). The 2024 annual runoff was near normal (17,920 m^3s^{-1}, +0.1 SD; Figure 7) as was the stratification at Rimouski station (-0.3 SD; Figure 8).

Stratification at Station 27 was above normal in 2024 (+1.1 SD; Figure 8). Although it was only slightly above normal at the Halifax 2 station (+0.6 SD), it was fourth highest averaged annually over the Scotian Shelf as a whole (+1.6 SD). Since 1948, there has been an increase in the mean stratification on the Scotian Shelf, resulting in a change in the 0–50 m density difference of 0.38 kg m^{-3} per 50 years (Figure 8). This change in mean stratification is due mainly to a decrease in the surface density, caused equally by warming and freshening.

2.7 CONDITIONS AT AZMP HIGH FREQUENCY SAMPLING STATIONS

At the high-frequency sampling sites (Figure 9), seasonal average 0–50 m temperature was above normal at all sites. Bottom temperature was below normal at Halifax 2 for the first time since 2011, consistent with the cooling of deep waters in the zone. It was above normal at all other sites, including a record high at Rimouski station where the cooling has not yet reached. Near-surface salinity (0–50 m) was normal at all sites except at Station 27 where it has been near to below normal for the last four years. Stratification, as stated above, was normal to above normal at all sites.

2.8 SUMMARY

Surface oceanic waters in the Atlantic zone during ice-free months have been mostly tracking the climate-change driven warming trends observed in the atmosphere. Sea surface temperatures averaged over the 2024 ice-free months were all above normal across the zone, with seasonal series records set in six areas. The last four years have been the 2nd to 5th warmest after the record of 2012.

Warming winters have also led to less sea ice cover and warmer and thinner cold intermediate layers. The period since 2018 has seen only near-normal to warmer-than-normal CIL conditions across the zone. In 2024, CIL conditions and bottom waters affected by the CIL were warmer than normal across the Gulf of St. Lawrence and the Newfoundland and Labrador Shelf, but the Scotian Shelf had a near-normal CIL volume.

Deep-water temperatures on the Scotian Shelf and Gulf of St. Lawrence had been greatly influenced by an increasing proportion of warm saline waters (related to the Gulf Stream) relative to cold fresh Labrador Water in recent years. However, the transport along the Scotian Shelf break was above normal in 2023 for the first time since 2011, indicating possible increased input of cold waters with high dissolved oxygen concentrations that may feed into the Gulf of St. Lawrence and Scotian Shelf at depth. This transport was at a record high in 2024. Below-CIL bottom temperatures have decreased except in 4V where they were already near normal in 2023. In most cases, the decrease is from record highs observed in 2022. In the northern Gulf, bottom temperatures deeper than 200 m decreased to 4th highest of the time

series. On the Scotian Shelf, below-CIL bottom temperatures remained near normal in regions 4V and 4X and have decreased to below normal for the first time since 2008 in region 4W.

Four annual composite index time series were constructed as the average of anomalies shown earlier and represent the state of different components of the system with each time series contribution shown as stacked bars (Figure 10). The components describe sea surface and bottom temperatures, as well as the cold intermediate layer and sea ice volume, which are both formed in winter. Two bottom temperature indices group areas with colder waters affected by CIL conditions and waters that are below the influence of the CIL. These four composite indices measure the overall state of the climate system with positive values representing warm conditions and negative representing cold conditions (e.g., less sea ice and smaller CIL areas and volumes are translated into positive anomalies). Cumulated indices also give a sense of the degree of coherence between the various metrics of the environmental conditions and different regions across the zone. Sea surface anomalies are weighted to their spatial area (although not by the numbers of months in the season) and all four panels are weighted for missing values. On average over the zone, conditions in 2024 were second highest for surface temperatures, and above normal for CIL and sea ice anomalies as well as for bottom temperatures influenced by the CIL. The first two have been above normal since 2020 and the third since 2018. Bottom temperatures below the influence of the CIL were near normal for the first time since 2013.

3. BIOGEOCHEMICAL ENVIRONMENT

Blais, M., Bélanger, D., Casault, B., Clay, S., Devred, E., Galbraith, P. S., Johnson, C. L., Maillet, G., and M. Ringuette.

Lower trophic level organisms include phytoplankton and zooplankton. Together, they form the component of marine food webs that channel the sun’s energy to higher trophic level animals such as shellfish (e.g., crabs, lobsters, scallops, and mussels), finfish (e.g., capelin, cod, herring, and halibut), marine mammals (e.g., seals and whales), reptiles (e.g., leatherback and loggerhead turtles) and seabirds. Phytoplankton are microscopic algae that form the base of the aquatic food web and occupy a position in the marine food web similar to that of plants on land. There is a wide variation in the size of phytoplankton, from the small flagellates (<5 µm) to the large diatoms (300–500 µm), with each taxon fulfilling a different ecological function. Phytoplankton are the primary food source for zooplankton, which are the critical link between phytoplankton and larger organisms. Zooplankton are a diverse group of small animals mostly ranging from 0.2 to 20 mm in length that primarily drift with ocean currents. The zooplankton community includes animals such as copepods, gelatinous filter feeders and predators, and ephemeral larval stages of bottom-dwelling and planktonic invertebrates (i.e., meroplankton). As with phytoplankton, there is a broad range of sizes of zooplankton. Smaller zooplankton species and developmental stages are the principal prey of larval fish, and larger copepods are prey for juvenile and adult fishes and some seabird and baleen whale species.

The productivity of marine ecosystems depends primarily on photosynthesis, the synthesis of organic matter from carbon dioxide and dissolved nutrients by phytoplankton. Light provides the energy necessary for the transformation of inorganic elements into organic matter. The growth rate of phytoplankton is dependent on temperature and on the availability of light and nutrients in the form of nitrogen (nitrate, nitrite, and ammonium), phosphorous (phosphate), and silica (silicate), with the latter being essential for diatom production. During springtime, phytoplankton biomass increases rapidly, reaching a period of maximum biomass known as the spring bloom. The spring bloom occurs primarily in near-surface waters when the upper water column stabilizes, light and nutrients are available, and grazing by zooplankton is still low. In fall, a

secondary bloom, usually less intense (i.e., lower biomass/shorter duration) than the spring bloom, can occur when upper water column stratification breaks down and nutrients are mixed into the surface layer. We report on the amount of nutrients available for phytoplankton, the concentration of chlorophyll *a* (a proxy for phytoplankton biomass), features of the spring and fall blooms in terms of timing and intensity, and the biomass and abundances of key zooplankton taxa based on the data available from 1998 to 2024.

Indices of nitrate inventories, phytoplankton biomass, features of the spring and fall phytoplankton bloom derived from satellite observations, and zooplankton abundance and biomass from the Labrador Sea (Ringuette et al. 2022), Newfoundland Shelf (Bélanger et al. 2024), Gulf of St. Lawrence (Blais et al. 2024) and Scotian Shelf (Casault et al. 2025) are summarized as time series of annual values in matrix form in Figure 11 to Figure 14. Anomalies were calculated using a climatological reference period of 1999–2020 for the biogeochemical parameters derived from in situ observations during seasonal oceanographic surveys. Unless otherwise noted, the regional citations provided above include the methodologies used in this current assessment. Descriptions of the aforementioned indices in 2024 will be published in similar regional reports.

In this report, characteristics of the phytoplankton blooms were derived from daily composites of chlorophyll *a* concentration at the ocean surface derived from the Ocean-Colour Climate Change Initiative (OC-CCI, 1998–2024) dataset provided by the Plymouth Marine Laboratory as recommended by the European Space Agency whereas previous reports used the Moderate Resolution Imaging Spectroradiometer (MODIS) “Aqua” sensor launched by National Aeronautics and Space Administration (NASA) in July 2002. The use of the OC-CCI product enhances zone coverage, which improves the accuracy of our estimates (Sathyendranath et al., 2019). However, it also causes changes in seasonal estimates and anomalies, which often differ from those reported in last year’s report using the MODIS ocean colour product. Also, the metrics used to characterize the timing and intensity of the bloom follow the method updated in the 2023 report, and include information on the fall bloom since the 2023 report. Intensity of the spring and fall blooms is expressed as the daily surface chlorophyll *a* concentration averaged over spring and fall seasons, respectively.

The 25-year time series of biogeochemical variables highlight the high degree of interannual variability of the lower trophic levels as compared to the physical variables. Even without long-term trends, distinct shifts for several biological variables are evident in recent years with the sign of anomalies persisting for several years. Moreover, a high degree of synchronicity in biological variability at adjacent locations can also be observed, although spatial variability may also be considerable in some instances.

3.1 NUTRIENTS

In the northwest Atlantic continental shelf waters, nitrate, the dominant form of nitrogen, is usually the limiting nutrient for phytoplankton growth. The subsurface nitrate inventory is the amount of nitrate generally contained in waters below the surface mixed layer (depths of 50–150 m for Labrador and Newfoundland Shelf, Gulf of St. Lawrence and Scotian Shelf, and depths deeper than 100 m for the Labrador Sea). Generally, this inventory is independent of phytoplankton growth, so it provides a good indicator of resources that can be mixed into the surface mixed layer during winter, or by upwelling during summer and fall, to become available for phytoplankton growth. Subsurface nitrate inventories, and the relative abundances of other nutrients, are mostly dependent on the source waters that make up the deep water (> 150 m) on continental shelves, which can vary from year to year. Subsurface nitrate inventories in 2024 showed lower-than-normal inventories in most regions including the Labrador Sea, most of the Gulf of St. Lawrence, and the Scotian Shelf, but higher-than-normal inventories on the

Newfoundland Shelf and the Grand Bank, resulting in a slightly negative zonal index (Figure 11). Subsurface nitrate inventories have generally been above normal over the past six years on the Newfoundland Shelf while below-normal nitrate inventories were observed in most years since 2016 in the Gulf of St. Lawrence and on the Scotian Shelf, and since 2019 in the Labrador Sea.

3.2 PHYTOPLANKTON

Chlorophyll *a* inventories in the upper ocean (0–100 m) are used as a proxy for the overall phytoplankton biomass. They exhibit a high degree of year-to-year variability (Figure 11). Part of this variation is explained by the timing of the program's oceanographic surveys throughout the zone relative to the timing of spring and fall phytoplankton blooms.

Annual chlorophyll *a* inventories in 2024 were mainly near normal in the Labrador Sea, on the Newfoundland Shelf and the Grand Banks, and in most of the Gulf of St. Lawrence. However, the St. Lawrence Estuary (Rimouski) and northwest Gulf showed strong positive anomalies. On the Scotian Shelf, easternmost sections were associated with strong negative anomalies, while westernmost sections showed above-normal chlorophyll *a* levels. The zonal annual chlorophyll *a* index was near normal (Figure 11). Anomalies of chlorophyll *a* have mostly been normal or above normal on the Newfoundland Shelf and in the Gulf of St. Lawrence since 2017. Although subsurface nutrient inventories provide some threshold to limit seasonal production dynamics across the zone, additional factors are likely to influence local nutrient-phytoplankton dynamics, such as the phytoplankton community composition and the variability of the nutrient transfer from the subsurface layer to the surface waters where phytoplankton production occurs. The balance of these factors is likely to differ when considered at the very large spatial scale from the Gulf of Maine to the Labrador Sea, which includes estuarine to oceanic environments.

The timing and intensity of the spring and fall phytoplankton blooms provide important information about regional variations in ecosystem productivity and are linked to the production of organisms that depend directly on lower trophic levels. Bloom intensity (i.e., chlorophyll biomass production) partly depends on the amount of nutrients that are mixed into surface waters over the course of the winter for the spring bloom, or through episodic upwellings or water column mixing events such as windstorms during fall. Peak biomass accumulation and bloom duration are also influenced by the extent of zooplankton grazing.

The timing of the 2024 spring phytoplankton bloom was generally earlier than normal, with particularly strong negative (i.e., early) anomalies in AR7W-West (record-early timing) and AR7W-Central (Figure 12). On the other hand, spring bloom timing was later than normal in AR7W-East and in the westernmost part of the Scotian Shelf and on Georges Bank. Spring bloom timing has generally been early in the Gulf of St. Lawrence since 2016. The intensity of the spring bloom has been dominated by interannual variability across the Atlantic zone over the time series, with little spatial coherence in anomaly patterns. While both above- and below-normal spring bloom intensities were observed in 2024, including intense spring blooms in Avalon Channel and a record-high value on St. Pierre Bank, the zonal spring bloom intensity index was near normal.

Around 2010, the timing of the fall bloom onset transitioned from mainly earlier to mainly later than normal in the Gulf of St. Lawrence and on the Scotian Shelf. The fall bloom timing was later than normal in 2024 in AR7W-East and AR7W-West, in the southernmost Newfoundland Shelf polygons and across the Gulf of St. Lawrence and Scotian Shelf (Figure 12). The timing was mostly earlier than normal elsewhere on the Newfoundland Shelf and in AR7W-Central. In 2024, two record-early timings were observed on the Newfoundland Shelf (Avalon Channel and Hibernia), while two record-late timings were observed (AR7W-West and eastern Scotian Shelf). Since 2016, most regions have exhibited above-normal fall surface chlorophyll *a* concentrations.

While anomalies remained positive in 2024 in most polygons of the Labrador Sea and Newfoundland Shelf, the fall chlorophyll *a* average was mainly near to below normal in the other regions (Figure 12).

3.3 ZOOPLANKTON

Zooplankton community structure is strongly influenced by depth, temperature and season, and the community's composition differs greatly among the northwest Atlantic bioregions. Despite regional composition and diversity differences, four indices of abundance provide good indicators of the state of the zooplankton community. Zooplankton abundance indices exhibited a high degree of large-scale coherence in their signal across different parts of the Atlantic zone (Figure 13). Copepods are by far the most abundant group, but non-copepods are also an important component of the zooplankton community in terms of abundance and ecological functions. Two copepod taxa are used to characterize trends in copepod groups representing different life history patterns: *Calanus finmarchicus* and *Pseudocalanus* spp. *Calanus finmarchicus* is a large, ubiquitous copepod that dominates zooplankton biomass throughout most of the zone. It develops large energy reserves in later developmental stages and is therefore a rich source of food for pelagic fish. *Pseudocalanus* spp. are small copepods that are widespread throughout the Atlantic zone and have smaller energy reserves relative to *C. finmarchicus*. Their life history features are generally representative of smaller taxa in the copepod community. We also report on the dry biomass of the zooplankton in the 0.2–10 mm size fraction, which is typically dominated by copepods (Figure 14).

A zooplankton community shift occurred around 2013–2014 across the Atlantic zone, characterized by lower zonal average abundances of the large copepod *C. finmarchicus*, and higher abundances of the small copepod *Pseudocalanus spp.* and non-copepods after 2013–2014. Although the abundance of *C. finmarchicus* was closer to normal between 2019 and 2022, the overall abundance of *Pseudocalanus* spp. and non-copepod zooplankton remained elevated during that period (Figure 13). 2024 was the second consecutive year in which zonal average conditions for most of the zooplankton indices returned to levels similar to those observed prior to the early 2010s. *Calanus finmarchicus* showed strong positive anomalies in several locations, including record-high values at Station 27, on the southeast Grand Banks and in the northeast Gulf, leading to the third highest zonal average abundance over the time series. Total copepod abundances were mainly above normal on the Newfoundland Shelf and Grand Bank, and below normal in the Gulf of St. Lawrence and on the Scotian Shelf, with a negative zonal index. *Pseudocalanus* spp. anomalies showed similar spatial patterns, except on the Scotian Shelf where they were mostly neutral. The abundance of *Pseudocalanus* spp. reached record-low values in the Estuary (Rimouski) and central Gulf of St. Lawrence, and a record high on the Halifax section, and the zonal average was near normal. The abundance of non-copepods continued the decade-long pattern of mostly positive anomalies across the Atlantic Zone that started in 2014.

Despite the general increase in *C. finmarchicus* abundances, zooplankton biomass remains mainly below normal in the Gulf of St. Lawrence and on the Scotian Shelf, including a record-low biomass at Cabot Strait. However, on the Newfoundland Shelf, zooplankton biomass was slightly above normal on most sections and strongly above normal on Seal Island section, continuing a pattern of primarily above-normal zooplankton biomass observed over almost a decade in this region (Figure 14). In the Gulf of St. Lawrence, the low zooplankton biomass in 2024 is largely due to low abundance of *Calanus hyperboreus,* an arctic *Calanus* species that is even larger than *C. finmarchicus* (not shown). Overall, the zonal index indicates lower-than-normal zooplankton biomass for the third year in a row, similar to the 2015–2017 period that was marked by very low zooplankton biomass throughout most of the Atlantic zone. Zonal biomass averages have been primarily below normal since 2010.

Recent findings in zooplankton community structure suggest that changes are taking place in the marine food web energy flow of the Atlantic Canadian waters (Blais et al. 2024, Casault et al. 2025, Bélanger et al. 2024). These changes are associated with shifts in the distribution of North Atlantic right whales in their northwest Atlantic shelf foraging areas (Brennan et al. 2021) and may be associated with declines in herring (Brosset et al. 2019) in the Atlantic zone. However, the broader consequences to the marine ecosystem are not yet fully characterized.

4. CHEMICAL OCEANOGRAPHIC CONDITIONS

Martine Lizotte, Marjolaine Blais, Lindsay Beazley, David Bélanger, Kumiko Azetsu-Scott, Benoit Casault, Joël Chassé, Frédéric Cyr, Alexandria Fudge, Carrie-Ellen Gabriel, Peter S. Galbraith, Anne-Josée Hébert, Gary Maillet, Shannah Rastin, Stephen Snook, Michel Starr

The global ocean is undergoing profound chemical changes driven by planetary climate and environmental alterations associated with anthropogenic activities (IPCC, 2021). Among the most significant of these changes are shifts in the cycling of elements such as carbon and oxygen, leading to ocean acidification (OA) and deoxygenation, both of which have far-reaching consequences for marine ecosystems and the services they provide (IPBES, 2019).

During the decade from 2014 to 2023, the global ocean has absorbed atmospheric CO_2 at a rate of 2.9 ± 0.4 gigatonnes of carbon per year, representing a sink for 26% of total CO_2 emissions (Friedlingstein et al., 2024). The uptake of anthropogenic CO_2 (C_{ant}) by the oceans, while mitigating some of the atmospheric CO_2 increase, triggers a series of chemical reactions that lower the concentration of bases in seawater and increase proton (H^+) concentrations, thereby raising “acidity levels” (Gattuso & Hansson, 2020). This process known as ocean acidification lowers the pH. The current rates of oceanic chemical changes due to C_{ant} are 100 times faster than those during the last glacial period. Globally, the surface ocean’s average pH has decreased by approximately 0.11 units between 1750 and 2000, resulting in a 30% increase in acidity (Friedrich et al., 2012; Caldeira & Wickett, 2003; Jiang et al., 2019; Orr et al., 2005). In Atlantic Canadian surface waters, pH is declining even faster, by 0.03–0.04 units per decade, compared to the global average pH decline of 0.017–0.027 units per decade (Bernier et al., 2023).

Beyond the surface of the ocean, the downward transport of C_{ant} is intensifying acidification in the ocean interior, reaching depths of hundreds to thousands of meters (Müller & Gruber, 2024). In some regions, sub-pycnocline waters are acidifying faster than surface layers (Lauvset et al. 2020; Fassbender et al., 2023). While C_{ant} accumulation is the primary driver of ocean interior acidification, variable rates of CO_2-carbonate system changes can also arise from water mass redistributions and changing physical oceanographic conditions (Chen et al., 2017; Gruber et al., 2019; Müller & Gruber, 2024). Modifications in biological and carbonate pumps, including changes in organic matter production, remineralization, and $CaCO_3$ mineral production and dissolution, may further impact key carbon parameters like total dissolved inorganic carbon (DIC) and total alkalinity (TA) (Gruber et al., 2023). These modifications can be particularly important in nearshore waters and ocean margin areas, where acidification is exacerbated by shifts in coastal and estuarine hydrographic (*e.g.*, freshwater discharge) and biogeochemical processes (*e.g.*, atmospheric deposition, nutrient loading and resulting eutrophication and remineralization of organic matter) (Cai et al., 2021; Doney, 2010). The northwest Atlantic continental shelf is a region where many of these processes converge, though they do so in different ways across various areas. This convergence induces significant temporal and spatial variability in the CO_2-carbonate system. While historical data on acidification parameters exist in the Atlantic Zone (*e.g.*, Mucci et al., 2011), systematic measurements of OA parameters have

been ongoing since fall 2014 as part of the AZMP and the Aquatic Climate Change Adaptation Services Program of DFO (Gibb et al., 2023; Galbraith et al., 2024).

The simultaneous alterations in seawater chemistry ([H^+], [CO_2], bicarbonate [HCO_3^-], and carbonate [CO_3^{2-}]) associated with OA have complex and multifaceted effects on marine organism and ecosystem functions (Doney et al., 2020, Figuerola et al., 2021, Leung et al., 2022). Among these, reductions in the saturation state (Ω) of calcium carbonate ($CaCO_3$) minerals, such as calcite (Ω_C) and aragonite (Ω_A) below critical thresholds may impact marine organisms that build shells, skeletons, and structures from $CaCO_3$, such as mollusks, crustaceans and corals. This is largely due to the increased energetic costs required to sustain net calcification under acidic conditions (Kroeker et al., 2010, 2013; Clements & Hunt, 2017, 2018; Rheuban et al., 2018; Pousse et al., 2020). In addition, modifications in pH can directly impact physiological processes that rely on the transfer of protons (H^+), including olfactory senses in fish (e.g., Dixson et al., 2015), and biomineralization in calcifying organisms (Jokiel, 2011, 2013; Thomsen et al., 2015; Toyofuku et al., 2017). Finally, a growing issue is the rise in water volumes with *in situ* partial pressure of CO_2 (pCO_2) surpassing 1,000 µatm, a condition termed ocean hypercapnia (McNeil & Sasse, 2016). Ocean hypercapnia adversely affects the physiological, behavioural, and neurological functions of marine organisms by impairing their ability to expel CO_2 during respiration and disrupting their internal acid-base balance (Nilsson et al., 2012; Perry & Gilmour, 2006; Pimentel et al., 2016; Feely et al., 2018). The increasing frequency and extent of ocean interior acidification and hypercapnic conditions may have detrimental implications for mesopelagic fisheries (Fassbender et al., 2023), including those in the North Atlantic Zone. Fluctuations in each of these CO_2-carbonate system variables can cause stress for marine organisms and may be compounded by concurrent stressors including, but not limited to, temperature fluctuations and oxygen availability (Kroeker et al., 2013; Arroyo et al., 2022).

The global ocean has lost about 2% of its oxygen content over the past 50 years (Schmidtko et al., 2017), with deoxygenation rates in the nearshore waters of the northwest Atlantic exceeding the global average (Gilbert et al., 2010). This oxygen loss spans estuaries, coastal waters, semi-enclosed seas, and the open ocean (Diaz et al., 2019; Falkowski et al., 2011; Limburg et al., 2020). Primarily driven by increased ocean warming and stratification, and changes in ocean circulation (Claret et al., 2018, Jutras et al., 2023), deoxygenation also results from modifications in ocean biogeochemistry associated with eutrophication and organic matter remineralization, particularly in coastal, near-shore, and ocean margin areas (Keeling et al., 2010; Levin, 2018; Oschlies et al., 2018; Rabalais, 2019). Reductions in oxygen levels can cause significant alterations in the range of habitats for marine organisms, as well as modifications in oceanic productivity, biodiversity, and biogeochemical cycling (Breitburg et al., 2018). Deoxygenation has been shown to affect biological systems at all levels, from cells and organs, to individuals, populations, communities, and ecosystems (Roman et al., 2024; Woods et al., 2022). Additionally, deoxygenation through microbial respiration can exacerbate ocean acidification via the accumulation of metabolic CO_2, a phenomenon frequently observed in deep waters (*e.g.*, Gobler & Baumann, 2016; Mucci et al., 2011; Arroyo et al., 2022).

4.1 DISSOLVED OXYGEN SATURATION

Oxygen tolerance of marine organisms widely varies and because temperature influences the oxygen solubility, thresholds reflecting organism tolerances are generally better expressed in terms of oxygen saturation rather than oxygen concentration (Breitburg et al., 2018; Vaquer-Sunyer & Duarte, 2008). In the nearshore waters of the northwest Atlantic Ocean, the hypoxia threshold is generally set at 30% oxygen saturation (≈ 100 µmol L^{-1}), although the more

sensitive organisms may express a reduction in metabolic functions when saturation levels decrease below 70% (≈ 215 µmol L^{-1}; Plante et al., 1998; Chabot & Dutil, 1999; Chabot & Claireaux, 2008; Brennan et al., 2016).

Dissolved oxygen saturations are generally above the 70% metabolic threshold across the zone over the time series, except for the near-bottom waters of the deep channels of the Gulf of St. Lawrence, starting from Cabot Strait, and for the Halifax-2 coastal station. As deep waters slowly flow from the mouth of the Laurentian Channel to its head in the St. Lawrence Estuary, the dissolved oxygen content gradually decreases due to microbial respiration and the oxidation of sinking organic material. Consequently, the deepest waters of the estuary, particularly at the head of the Laurentian Channel, exhibit the lowest oxygen levels. In this area, dissolved oxygen levels ranged between 30 and 40% in the early 1970s and have consistently been hypoxic (below 30%) since 1984 (Gilbert et al., 2005, Blais et al. 2024).

Various factors may have driven the decadal alterations in dissolved oxygen concentration and saturation within the deep waters of the Gulf of St. Lawrence. Variations in the relative contributions of oxygen-rich Labrador Current Water (LCW) and oxygen-poor North Atlantic Central Waters (NACW) entering the Laurentian Channel could have exerted a predominant influence (Gilbert et al., 2005). Sudden swift reductions in oxygen levels observed since ca. 2016 in the deep waters of the Gulf of St. Lawrence could have arisen from a diminished influx of highly oxygenated LCW into the deep waters of the system, favouring the influx of low-oxygenated NACW (Jutras et al., 2020). These circulation alterations also likely accounted for the rapid rise in deep bottom temperatures in the Gulf of St. Lawrence and Estuary (Chapter 2). Part of the oxygen depletion likely stemmed from enhanced oxygen utilization in response to elevated temperatures and eutrophication in the St. Lawrence Estuary, as oxygen loss rates appear to exceed those expected from changes in water mass composition (Gilbert et al., 2005; Blais et al., 2024; Jutras et al., 2023).

In 2024, oxygen saturation stayed above or very close to the metabolic threshold in most locations of the Atlantic Zone (Figure 15). However, in the deep near-bottom waters of the Laurentian channel, the oxygen saturation levels were mostly below 50% in the easternmost locations, decreasing to 30% and below in the northwest Gulf and the Estuary. This represents a significant decline compared to 2018, when saturation levels <30% were only observed at Rimouski station. At this station, the annual average oxygen saturation in the near-bottom waters was 11% in 2024, similar to the 2023 average and only slightly above the record low of 10% set in 2022 (Figure 15). The historical lowest monthly average of oxygen saturation was also recorded in 2022 at Rimouski station, when the bottom 50 m of the water column remained consistently below 11% throughout the fall (Figure 16). Although the monthly means of oxygen saturation in the bottom waters of Station 27 in 2024 were mostly below the climatology, they remained above 80% and within the bounds of the series range (Figure 16).

4.2 CO_2-CARBONATE SYSTEM

4.2.1 Inorganic carbon state variables

Variations in ocean inorganic carbon state variables (total alkalinity (TA) and total dissolved inorganic carbon (DIC)) provide insight into the ocean's buffering capacity against acidification, the overall health of marine ecosystems, and the dynamics of the carbon cycle. Total alkalinity is defined as the excess of proton acceptors over proton donors. Higher TA levels generally indicate a greater ability to neutralize acidity, which is crucial for maintaining stable pH levels amid rising atmospheric and ocean metabolic CO_2. Total dissolved inorganic carbon is the sum of all dissolved inorganic carbon species contents ($[CO_{2(aq)}]$, $[H_2CO_3]$, $[HCO_3^-]$, and $[CO_3^{2-}]$). Monitoring DIC provides insights into how carbon is transported and transformed within the

North Atlantic Zone, which is crucial for assessing water quality changes driven by factors such as freshwater input, nutrient loading, organic matter decomposition, among other processes.

Average values of near-bottom TA on the Newfoundland and southern Labrador shelf sections exhibit the most stability, with the weakest zonal interannual variability and relatively low climatological standard deviations (ranging from ca. 2 to 5 μmol kg^{-1}; Figure 15). Annual averages of TA have been normal to below normal in all sections of the Newfoundland and Labrador region since 2021 (except for Bonavista in 2022). Zonally, lowest near-bottom TA levels (climatological mean of 2224 ± 5 μmol kg^{-1}) are found at Station 27, suggesting that these waters are less buffered against potential additions of C_{ant} and metabolic CO_2. Since 2020, TA anomalies in the Gulf of St. Lawrence region have generally been normal to above normal. Station Rimouski has exhibited neutral to positive anomalies in average annual TA since 2018. Apparent variability in TA anomalies in the Maritimes region could be related to greater variability in temporal coverage throughout the time series in the region that may challenge the computation of annual averages.

Unlike the relatively straightforward processes shaping TA in surface open-ocean waters, ocean margin areas—including estuaries, continental shelves, and upper slopes—are influenced by more complex TA sinks and sources (Cai et al., 2010). At depth, this complexity may result from upwelling of deep water enriched with alkalinity through enhanced carbonate mineral dissolution (Millero et al., 1998), removal through biological calcification (Cai, 2003; Cai et al., 2010), and TA production via anaerobic organic matter degradation in nearby sediments (***e.g.***, Chen & Wang, 1999; Fennel & Wilkin, 2009; Wang & Cai, 2004). Finally, although research remains limited, dissolved organic matter (DOM) may contribute to TA in some environments, especially where higher concentrations of its recalcitrant fraction are present at depth (Lee et al., 2024).

Average annual DIC anomalies in near-bottom waters of the Gulf of St. Lawrence and Maritimes regions have been predominantly above (Figure 15). Zonally, the highest annual concentrations of near-bottom DIC (above 2200 μmol kg^{-1}) are found in the Gulf of St. Lawrence. Notably, within this region, Rimouski station has experienced the strongest positive deviations from its climatology since 2020 with record-high annual DIC in 2023. Most Maritimes sub-regions, excluding the Halifax line, have exhibited strong positive annual DIC anomalies with record-high near-bottom DIC values in 2022 in Louisbourg and Browns Bank. In the Newfoundland and Labrador region, near-bottom DIC has been normal to above normal since 2022, culminating in a record-high anomaly at Station 27 in 2024.

4.2.2 Potential of hydrogen (pH)

The pH measures the potential of hydrogen ions (H^+) or the “acidity level” of seawater, expressed on a logarithmic scale. When employed, terms like “more acidic” or “acidification” indicate increasing H^+ levels. In reality, oceanic waters are typically mildly alkaline with pH> 7.0, as genuinely acidic conditions (pH <7.0) are rarely encountered in marine systems. Throughout this document, pH is expressed on the total hydrogen ion scale (pH_T), unless otherwise specified.

Since 2020, annual averages of near-bottom water pH_T have been mostly normal to below normal across the Atlantic Zone (Figure 17). A marked shift towards acidification has emerged in the Gulf of St. Lawrence region, particularly at Station Rimouski, where monthly near-bottom pH_T has deviated from the historical average (Figure 16). A significant declining trend in pH_T has been observed between 2014 and 2024 in near-bottom waters at Station Rimouski with a rate of -0.0057 units $year^{-1}$ ($p < 0.001$), equating to a 1.3% annual increase in acidity.

Interannual variations of near-bottom pH_T are typically strongest throughout the time series in Newfoundland shelf cross sections and at Station 27, making it more difficult to identify clear

long-term trends in those areas. Nevertheless, despite this interannual variability, the regression line fitted to the monthly average time series at Station 27 indicates a significant ($p < 0.001$) declining trend in near-bottom pH_T values of -0.0095 units year^{-1} between 2014 and 2024 (Figure 16). This represents an average 2.2% increase in acidity per year over the timespan of observations. Near-bottom waters at both high frequency stations are acidifying faster (-0.0057 and -0.0095 units of pH year^{-1} at Station Rimouski and Station 27, respectively) than global basin-scale surface waters, where rates range from -0.0013 to -0.0025 units year^{-1} for the 1982–2012 reference period (Bates et al., 2014) and -0.0017 units year^{-1} for the 1985–2022 reference period (CMEMS, 2025). This suggests an amplification of interior OA at these stations. Monthly pH_T variability is more pronounced in surface waters (Figure 16), driven by factors that include seasonal changes in primary production, air-sea gas exchange, riverine inputs, and oceanographic processes like mixing and upwelling. No statistically significant decreases in surface pH_T values have been observed at Station Rimouski and Station 27 over the past decade. In 2024, with the exception of the Northeast Gulf and Browns Bank, all subregions of the Atlantic Zone recorded negative annual pH_T anomalies in near-bottom waters, with a time series record low of 7.91 at Station 27.

4.2.3 Partial pressure of CO_2

Ocean hypercapnia, which refers to elevated levels of CO_2 in seawater, can significantly impact marine organisms by affecting their physiology, behaviour, growth, reproduction, and survival (*e.g.*, Michaelidis et al., 2005; Munday et al., 2009; Heuer & Grosell, 2014). While direct pCO_2 measurements are crucial for understanding changing ocean interior levels of CO_2, it is important to recognize that estimates derived from other CO_2-carbonate system parameters (pH_T, TA and DIC, such as in this report) carry greater uncertainty, especially at depths below 100 m (Weiss, 1974; Orr et al., 2015).

Climatological near-bottom pCO_2 mean values vary ca. 3-fold across the NW Atlantic sub-regions for the 2014–2024 time series shown in Figure 15. Regionally, lowest and highest pCO_2 values are found in Newfoundland and Labrador and Gulf of St. Lawrence regions, respectively. Since 2020, annual pCO_2 averages have exhibited normal or below normal conditions across sections of the Maritimes and Newfoundland and Labrador regions, as well as in subregions of the Gulf of St. Lawrence. Near-bottom waters of the Estuary (including Station Rimouski) have been consistently hypercapnic ($pCO_2 > 1{,}000$ µatm) since carbonate system measurements began in 2014. The Estuary is also host to the largest interannual variability in near-bottom pCO_2, reflective of the complex carbonate chemistry dynamics typical of estuarine environments (Cai et al., 2021). Near bottom water hypercapnic conditions have also been observed in the northwest Gulf (since 2020) and in the Northeast Gulf (in 2022 and 2023). In 2024, near-bottom waters of the Centre Gulf and Cabot Strait subregions are approaching hypercapnic conditions, with 834 and 825 µatm, respectively. As a semi-enclosed oceanic region, the Gulf of St. Lawrence shows more pronounced acidification, consistent with observations that ocean margin areas may be more impacted by the phenomenon than open-ocean basins (Lee et al., 2011). While C_{ant} is continuously imported at depth, particularly from the North Atlantic through Cabot Strait, accumulation of metabolic CO_2 is also contributing to the long-term carbon build-up in near-bottom waters of the basin.

4.2.4 Calcium carbonate saturation states and substrate-inhibitor ratio

The saturation state of $CaCO_3$ minerals (Ω_{CaCO3}) is a dimensionless ratio comparing the concentration of dissolved $CaCO_3$ ions in seawater to their saturation concentration. It serves as a metric for dissolution thermodynamics: when $\Omega < 1$, dissolution of unprotected biogenic $CaCO_3$ structures is thermodynamically favoured (Morse et al., 2007). Biogenic $CaCO_3$ exists primarily as calcite or aragonite, which differ in crystal structure and solubility (Mann, 2001). Calcite is

mainly produced by coccolithophores, foraminifera, and some crustaceans, while aragonite is typically found in scleractinian corals and pteropods. Mollusks can form both calcite and aragonite, and echinoderms produce calcite that includes significant magnesium (Mg) within the crystal lattice (Mann, 2001; Bach, 2015). Aragonite's higher solubility generally results in lower saturation states in seawater compared to calcite, making aragonite-dependent marine organisms more susceptible to dissolution under changing ocean chemistry. Evidence shows that commercially important marine bivalves and crustaceans experience acute or chronic responses to OA when Ω levels range between 1.0 and 2.0. This section reports on two key thresholds: Ω <1.0, indicating conditions that favour dissolution, and a conservative biological threshold of Ω <1.5, considered suboptimal for marine organisms due to its association with observed physiological effects (Gazeau et al., 2013; Waldbusser & Salisbury, 2014; Dixson et al., 2010; Keppel et al., 2012; Long et al., 2016; Rodriguez-Dominguez et al., 2018; Siedlecki et al., 2021).

While dissolution due to acidification is primarily an inorganic process linked to undersaturation states of $CaCO_3$ minerals, marine calcification is biologically mediated and more complex. Biocalcification typically involves uptake of calcium ions (Ca^{2+}) and bicarbonate ions (HCO_3^-) as substrates (Allemand et al., 2004; Cyronak et al., 2016; Kahil et al., 2021; Mackinder et al., 2010; Mann, 2001; Stumpp et al., 2012). The processes of biocalcification vary widely across taxa, each with unique mechanisms for inorganic carbon uptake and varying sensitivities to H^+ (Mann, 2001). This inherent complexity makes it challenging to predict the net response of marine calcifiers based solely on the variability in the Ω metric (Bach, 2015; Ninokawa et al., 2024). The substrate-inhibitor ratio (SIR), defined as the ratio of the substrate ($[HCO_3^-]$) to the waste product ($[H^+]$), has been proposed as an additional metric to assess the influence of changing carbonate chemistry on biocalcification (Bach, 2015). In this report, while pH is presented on the total scale, the hydrogen ion concentrations in the $[HCO_3^-]/[H^+]$ ratio are on the free scale (SIR in mol:µmol), which better reflects the ionic environment experienced by marine organisms. A higher SIR indicates more favourable conditions for calcification (Bach, 2015; Jokiel et al., 2011; Cyronak et al., 2016; Roleda et al., 2012). Although SIR offers a straightforward numerical measure to understand $CaCO_3$ production and the effects of varying chemical conditions on calcifying organisms, it does not entirely capture the intricate interactions among carbonate system variables that are believed to influence calcification, as noted by others (Ninokawa et al., 2024).

Annual averages of near-bottom water Ω_A have been below the critical threshold of 1.5 since 2015 in all sections of the Newfoundland and Labrador and Maritimes regions, except for Browns Bank, for which annual average Ω_A values have oscillated between 1.37 to 1.91 since 2014 (Figure 17). In all areas of the Gulf of St. Lawrence, including at the high frequency Station Rimouski, near-bottom water values of Ω_A have been consistently undersaturated (Ω_A <1.0) since 2017, with sustained desaturation (negative anomalies) since 2020 in the Estuary and northwest Gulf. Annual averages of near-bottom water Ω_A have been at or below-normal conditions across most Maritimes and Newfoundland and Labrador sections since 2022. In 2024, the annual average Ω_A in near-bottom waters at Station 27 crossed, for the first time, the undersaturation threshold (Ω_A = 0.99). The 2024 Ω_A conditions in near-bottom waters of the Gulf of St. Lawrence subregions were all undersaturated, particularly in the Estuary and at Station Rimouski with Ω_A values of 0.59 and 0.58, respectively, representing a ca. 12–13% decline relative to 2007 levels ($\Omega_A \approx 0.67 \pm 0.03$, see Mucci et al., 2011).

Zonal patterns of annual anomalies of near-bottom Ω_C and Ω_A are similar in their overall trends. While Ω_C has not fallen below the critical 1.5 threshold in the Maritimes and Newfoundland and Labrador regions, the 2024 annual Ω_C average at Station 27, has shown the strongest negative anomaly of the series (record low Ω_C of 1.59). In the Maritimes region, the Louisbourg section

has exhibited mostly negative annual Ω_C average anomalies since 2017, and values at Cabot Strait have been consistently below normal since 2020. Most areas of the Gulf of St. Lawrence region, except for the Centre Gulf, have been under the 1.5 threshold since 2015. Notably, the Estuary and Station Rimouski have experienced persistent calcite undersaturation (Ω_C <1.0) since 2020 and 2019, respectively. In 2024, the annual averages of Ω_C in near-bottom waters of the Estuary and at Station Rimouski were undersaturated at 0.94 and 0.92, respectively, representing an overall ca. 12–13% decline from 2007 values ($\Omega_A \approx 1.06 \pm 0.04$, see Mucci et al. 2011). The observed expansion of both Ω_A and Ω_C undersaturation in bottom waters of the St. Lawrence Estuary aligns with modelling projections of time-of-emergence for carbonate system changes (Lavoie et al., 2020).

Annual averages of SIR ($[HCO_3^-]/[H^+]$ in mol μmol^{-1}) show considerable spatial variability, with a more than two-fold difference in climatological values between regions (ranging from 0.092 to 0.250 mol μmol^{-1}, Figure 17). Calcification in certain marine organisms may drastically decline below a critical threshold equivalent to an SIR of 0.100 mol μmol^{-1} (Thomsen et al., 2015). This implies that near-bottom waters of the Gulf of St. Lawrence region that are already under or nearing this SIR threshold present a combination of co-occurring dissolution/biomineralization stressors (*i.e.*, low Ω_{CaCO3} and low SIR). Overall, higher SIR values (mostly $>$0.2 mol μmol^{-1}) found in the Maritimes and Newfoundland and Labrador regions suggest more favourable conditions for biomineralization in near-bottom waters compared to the Gulf of St. Lawrence region, with values at the mid-range of oceanic SIR values (*e.g.*, ca from 0.050 to 0.350 mol μmol^{-1}, see Bach, 2015). Since 2020, annual averages of SIR have been normal to below normal in all subregions of the Gulf of St. Lawrence and Newfoundland and Labrador. In the Maritimes region, lowest annual values of SIR are found in the Cabot Strait section, with values consistently below 0.170 mol μmol^{-1}, while the Browns Bank section has exhibited persistent negative anomalies since 2019. In 2024, SIR values showed a decreasing gradient from Centre Gulf (0.141 mol μmol^{-1}) to Northeast Gulf (0.129 mol μmol^{-1}), to northwest Gulf (0.103 mol μmol^{-1}), and down to the Estuary (0.088 mol μmol^{-1}).

5. CONCLUSION

While a shift to warmer ocean conditions occurred prior to the implementation of the AZMP, the period since 2010 has seen further warming with sea surface temperatures reaching record values across the zone during various years since 2012, including in six of our reporting areas in 2024. In 2024, the winter average sea ice volume was at a record low in the Gulf of St. Lawrence and sea ice conditions were below normal on the Newfoundland and Labrador shelf. The summer cold intermediate layer areas measured at four sections on the Newfoundland and Labrador shelf were all below normal. Its volume was fifth smallest in the Gulf of St. Lawrence, but near normal on the Scotian Shelf. Bottom temperatures in areas affected by the CIL were above normal in all regions of the Newfoundland and Labrador Shelf and Gulf of St. Lawrence. Bottom temperatures in the deep channels of the Gulf of St. Lawrence and the Scotian Shelf, which are affected by the mixture of cold, fresh and warm, saline waters, show decreases from the 2022 record highs. In the Gulf of St. Lawrence, temperatures decreased to values similar to those of 2020. On the Scotian Shelf, they have decreased to near normal in regions 4V and 4X and even to below normal for the first time since 2008 in region 4W.

Patterns of variation in biogeochemical variables were dominated by short-term fluctuations (1 to 5 years) over the course of the 25-year time series, and many demonstrated some spatial structure across the Atlantic Zone. While short-term fluctuations in certain indices (e.g., *Calanus finmarchicus*, non-copepods) exhibit regionally coherent patterns across the Atlantic Zone, other indices (such as nitrate inventories and zooplankton biomass) have contrasting regional patterns. These differences underscore the influence of zonal scale environmental

gradients and oceanographic features that can affect lower trophic level responses differently across the Atlantic shelf bioregions. Overall, changes in the biogeochemical variables provide evidence for changes in the productivity and phenology of lower trophic levels in recent years, highlighted especially by a longer phytoplankton production season, which begins earlier in spring in some regions and later in fall in most of the Atlantic Zone, accompanied by lower nitrate subsurface inventories in some regions, and changes in the zooplankton community across the zone. Following a decade-long period of general decline in overall zooplankton biomass associated with lower abundances of *C. finmarchicus* and higher abundances of *Pseudocalanus* spp. that suggested a community shift to dominance of smaller copepods, an indicator of less efficient transfer of energy to higher trophic levels. High levels of phytoplankton biomass during fall and high abundance of *C. finmarchicus* in 2024 moderated this pattern and might suggest changes in the seasonality of lower trophic level production. However, zooplankton biomass in 2024 remained similar to the 2015–2017 low production potential period.

The North Atlantic zone is experiencing changes in its chemical conditions driven by alterations in hydrographic and biogeochemical processes that may impact the health and resilience of marine ecosystems. While oxygen saturation in deep near-bottom waters remained above the metabolic threshold of 70% in most locations of the North Atlantic zone in 2024, hypoxic conditions (<30%) have been prevalent in the Estuary and northwest Gulf of St. Lawrence since 2015 and 2020, respectively. The proportionally greater influx of oxygen-poor NACW and reduced contributions from oxygen-rich LCW in the deep waters of the Laurentian Channel in recent years, coupled with increased microbial respiration under warmer temperatures, have exacerbated oxygen depletion and the accumulation of metabolic CO_2. Hypercapnic conditions (P_{CO_2} >1,000 µatm) have been widespread in near-bottom waters of the St. Lawrence Estuary and northwest Gulf since 2014 and 2020, respectively. Over the North Atlantic zone, the downward transport of anthropogenic CO_2 is also intensifying acidification in the ocean interior, leading to higher decreasing rates of pH compared to other parts of the world ocean. Near-bottom water pH levels were below normal across most regions of the Atlantic Zone in 2024, with a record-low value at Station 27. Overall, there has been a broad trend of normal to deteriorating conditions for proxies of calcium carbonate biocalcification and dissolution in deep near-bottom waters of the North Atlantic zone since 2020. This is particularly evident in aragonite saturation states, which were below the dissolution threshold (Ω_A <1) across all subregions of the Gulf of St. Lawrence and fell below this threshold for the first time in 2024 at Station 27 and in Cabot Strait.

5.1 SUMMARY

- Monthly average sea surface temperatures were generally above normal from March through November, including 19 regional monthly record highs scattered throughout all regions except 4X and 5Ze. The Scotian Shelf (in December) and the Gulf of Maine (in February and December) had the only monthly average SSTs that were colder than normal. Sea surface temperatures are based on a new product for this report and some previously reported records have changed. However, the overall patterns remain the same.
- Sea surface temperature seasonal averages were above normal across the zone, reaching record highs in parts of the Newfoundland Shelf (3K, 3L, 3N), over the entire Gulf of St. Lawrence and east of Cape Breton (4Vn). The 2024 spatially weighted zonal average was second highest of the time series, with 2012 ranking first.
- Transport was normal along the Newfoundland and Labrador Shelf break, but at a record high along the Scotian Shelf break. This indicates increased input of cold and low salinity

waters with high dissolved oxygen concentrations that may feed into the Gulf of St. Lawrence and Scotian Shelf at depth.

- Winter average sea ice conditions were below normal on Newfoundland and Labrador Shelf and at a record low in the Gulf of St. Lawrence. In the 15-year period between 2010 and 2024, the Gulf of St. Lawrence seasonal average sea ice volume had 11 of the 15 lowest values in the 56-year time series.
- The cold intermediate layer (CIL) indices indicated warmer than normal conditions in the Gulf of St. Lawrence and on the Newfoundland and Labrador Shelf, and normal on the Scotian Shelf. The last time that colder than normal conditions occurred was in 2017 on the Newfoundland and Labrador Shelf, 2014 in the Gulf of St. Lawrence and 2008 on the Scotian Shelf.
- Bottom temperatures in areas affected by the CIL were above normal in all regions of the Newfoundland and Labrador Shelf and Gulf of St. Lawrence.
- Bottom temperatures in the deep channels of the Gulf of St. Lawrence and the Scotian Shelf, which are affected by the mixture of cold, fresh Labrador Current water and warm, saline waters related to Gulf Stream waters, show decreases from the 2022 record highs to values similar to those of 2020. On the Scotian Shelf, these bottom temperatures remained near normal in regions 4V and 4X and have decreased to below normal for the first time since 2008 in region 4W. The zonal average index was near normal for the first time since 2013.
- At the high-frequency sampling stations (Figure 1):
  - Seasonal average 0–50 m temperature was above normal at all sites.
  - Bottom temperature was below normal at Halifax 2 for the first time since 2011, consistent with the cooling of deep waters in the zone. They were above normal at all other sites, including a record high at Rimouski station where the cooling has not yet reached.
  - Near-surface salinity (0–50 m) was normal at all sites except at Station 27 where it was below normal.
  - Stratification was normal to above normal at all sites. Although it was only slightly above normal at Halifax 2, it was fourth highest averaged annually over the Scotian Shelf as a whole.
- Subsurface nitrate inventories were above normal on the Newfoundland Shelf and mostly below normal elsewhere. Inventories have been below average in the Gulf of St. Lawrence and on the Scotian Shelf since 2016 and in the Labrador Sea since 2019, but near or above normal on the Newfoundland Shelf since 2019.
- Chlorophyll *a* inventories were relatively normal in the Atlantic Zone, but well above normal at Rimouski Station and in the northwest Gulf of St. Lawrence, and well below normal on the eastern Scotian Shelf. Since 2017, inventories have been mostly normal or above normal on the Newfoundland Shelf and in the Gulf of St. Lawrence.
- The timing of the spring phytoplankton bloom peak was mostly earlier than normal, with record-early timing at AR7W-West. Spring bloom timing has generally been earlier than normal in the Gulf of St. Lawrence since 2016.

- Mean spring surface chlorophyll *a* concentration varied widely but were higher than normal in Avalon Channel and on St. Pierre Bank (record high), while most other locations had normal to below normal concentrations.
- The timing of the fall bloom onset was generally later than normal, except on most of the Newfoundland Shelf and in the AR7W-Central region. Two record-early timings were observed on the Newfoundland Shelf, while record-late timings occurred in the AR7W-West region and on the eastern Scotian Shelf.
- Since 2016, most regions have shown above-normal fall surface chlorophyll *a* averages. Averages in the Labrador Sea and Newfoundland Shelf were above normal in 2024, while they were near or below normal in the other regions.
- Total copepod abundances were mostly above normal on the Newfoundland Shelf, and below normal in the Gulf of St. Lawrence and on the Scotian Shelf.
- The abundance of non-copepods, although near normal, continued a decade-long above normal pattern across the Atlantic Zone.
- *Pseudocalanus* spp. abundance showed contrasting regional patterns, being above normal on the Newfoundland Shelf and below normal in the Gulf of St. Lawrence (record-low abundances at Rimouski station and in Centre Gulf). They were near normal on the Scotian Shelf, with the exception of a record high on Halifax Line.
- The abundance of *C. finmarchicus* was above normal at several locations, particularly in the Newfoundland Shelf and Gulf regions, with record-high abundances at Station 27, southeast Grand Banks and northeast Gulf of St. Lawrence. This marks a second consecutive year of widespread above normal abundances after a decade of near to below-normal abundances.
- Zooplankton biomass was mainly below normal in the Gulf of St. Lawrence and on the Scotian Shelf, with a record low at Cabot Strait, but above normal on the Newfoundland Shelf, continuing a decade-long trend.
- The near-bottom waters of the St. Lawrence Estuary remained in a state of severe dissolved oxygen undersaturation (<20%), and values at Station Rimouski were close to the 2022 record low.
- Hypercapnic conditions (pCO_2 > 1,000 µatm) have been prevalent in near-bottom waters of the St. Lawrence Estuary since 2014 and have extended to the northwest Gulf of St. Lawrence since 2020.
- All subregions of the Atlantic Zone recorded below normal annual pH_T in near-bottom waters, with a record low at Station 27, except in the northeast Gulf of St. Lawrence and on Browns Bank where values were near normal. A significant declining trend in pH_T has been observed over the recent decade (2014–2024) in near-bottom waters of both Station 27 and Rimouski Station.
- Near-bottom water aragonite saturation states were below the dissolution threshold (Ω_A <1) across all the subregions of the Gulf of St. Lawrence and fell below this threshold for the first time at Station 27 and in Cabot Strait. Calcite saturation states (Ω_C <1) were below the dissolution threshold in the St. Lawrence Estuary, including at Rimouski Station.
- Near-bottom waters in all subregions of the Atlantic Zone exhibited below-normal values of the biomineralization proxy substrate-inhibitor ratio (SIR), except in the northeast Gulf of St. Lawrence and Bonavista where values were near normal. The near-bottom waters of the St.

Lawrence Estuary and Rimouski Station have been below the critical SIR threshold of 0.1 since 2020 and 2014, respectively.

ACKNOWLEDGMENTS

Denis Lefaivre contributed the data for runoff at Québec City. Nancy Chen provided the along-shelf transports. The authors thank the following reviewers: Charles Hannah, Charles Tilney and Dave Capelle. We also thank Caroline Lehoux as editor. This report would not be possible without the data acquisition, analysis, and quality control performed by AZMP technicians and professionals across the zone.

REFERENCES

Allemand, D., Ferrier-Pagès, C., Furla, P., Houlbrèque, F., Puverel, S., Reynaud, S., Tambutté, É., Tambutté, S., & Zoccola, D. 2004. Biomineralization in reef-building corals: From molecular mechanisms to environmental control. Comptes Rendus Palevol. 3(6-7): 453-467. https://doi.org/10.1016/j.crpv.2004.07.011.

Arroyo, M. C., Fassbender, A. J., Carter, B. R., Edwards, C. A., Fiechter, J., Norgaard, A., Feely, R. A. 2022. Dissimilar sensitivities of ocean acidification metrics to anthropogenic carbon accumulation in the Central North Pacific Ocean and California Current Large Marine Ecosystem. Geophysical Research Letters. 49: e2022GL097835. https://doi.org/10.1029/2022GL097835.

Bach L. T. 2015. Reconsidering the role of carbonate ion concentration in calcification by marine organisms. Biogeosciences. 12: 4939–4951. https://doi.org/10.5194/bg-12-4939-2015.

Bates, N. R., Astor, Y. M., Church, M. J., Currie, K., Dore, J. E., González-Dávila, M., Lorenzoni, L., Muller-Karger, F., Olafsson, J., Santana-Casiano, J. M. 2014. A time-series view of changing ocean chemistry due to ocean uptake of anthropogenic CO_2 and ocean acidification. Oceanography. 27(1) : 126–141. http://dx.doi.org/10.5670/oceanog.2014.16.

Bélanger, D., Maillet, G., Cyr, F., Doyle, G., Rastin, S., Ramsay, D., Dalton, B., and Pepin, P. 2024. Biogeochemical Oceanographic Conditions on the Newfoundland and Labrador Shelf during 2019 and 2020. DFO Can. Sci. Advis. Sec. Res. Doc. 2024/074. vi + 55 p.

Bernier, R. Y., Jamieson, R. E., Kelly, N. E., Lafleur, C., Moore, A. M. 2023. State of the Atlantic Ocean Synthesis Report. Canadian Technical Report of Fisheries and Aquatic Sciences, 3544: v + 219 p.

Blais, M., Galbraith, P. S., Lizotte, M., Clay, S. A., and Starr, M. 2024. Chemical and Biological Oceanographic Conditions in the Estuary and Gulf of St. Lawrence during 2023. Can. Tech. Rep. Hydrogr. Ocean Sci. 385 : v + 84 p.

Brennan, C. E., Maps, F., Gentleman, W.C., Lavoie, D., Chassé, J., Plourde, S. and C.L. Johnson. 2021. Ocean circulation changes drive shifts in *Calanus* abundance in North Atlantic right whale foraging habitat: A model comparison of cool and warm year scenarios. Prog. Oceanogr. 197:102629.

Breitburg, D., Levin, L. A., Oschlies, A., Grégoire, M., Chavez, F. P., Conley, D. J., Garçon, V., Gilbert, D., Gutiérrez, D., Isensee, K., Jacinto, G. S., Limburg, K. E., Montes, I., Naqvi, S. W. A., Pitcher, Rabalais, N. N., Roman, M. R.,Rose, K. A., Seibel, B. A., Telszewski, M., Yasuhara, M., Zhang, J. 2018. Declining oxygen in the global ocean and coastal waters. Science **359**, 46. https://doi.org/10.1126/science.aam7240

Brickman, D., Hebert, D., Wang, Z. 2018. Mechanism for the recent ocean warming events on the Scotian Shelf of eastern Canada. Continental Shelf Research, **156**: 11–22, https://doi.org/10.1016/j.csr.2018.01.001.

Brosset, P., Doniol-Vacroze, T., Swain, D.P., Lehoux, C., Van Bereven, E., Mbaye, B.C., Emond, K. and S. Plourde. 2019. Environmental variability controls recruitment but with different drivers among spawning components in Gulf of St. Lawrence herring stocks. Fish. Oceanogr. **28**:1-17.

Caldeira, K., Wickett, M. E. 2003. Oceanography: Anthropogenic carbon and ocean pH. Nature. 425(6956): 365. https://doi.org/10.1038/425365a.

Cai, W.-J. 2003. Riverine inorganic carbon flux and rate of biological uptake in the Mississippi River plume. Geophysical Research Letters. 30(2):1032. https://doi.org/10.1029/2002GL016312.

Cai, W.-J., Xu, Y.-Y., Feely, R. A., Wanninkhof, R., Jönsson, B., Alin, S. R., Barbero, L., Cross, J. N., Azetsu-Scott, K., Fassbender, A. J., Carter, B. R., Jiang, L.-Q., Pepin, P., Chen, B., Hussain, N., Reimer, J. J., Xue, L., Salisbury, J. E., Hernández-Ayón, J. M., Langdon, C., Li, Q., Sutton, A. J., Chen, C.-T. A., Gledhill, D. K. 2020. Controls on surface water carbonate chemistry along North American ocean margins. *Nature Communications*, **11**(1). https://doi.org/10.1038/s41467-020-16530-z.

Cai, W.-J., Feely, R. A., Testa, J. M., Li, M., Evans, W., Alin, S. R., Xu, Y.-Y., Pelletier, G., Ahmed, A., Greeley, D. J., Newton, J. A., Bednaršek, N. 2021. Natural and Anthropogenic Drivers of Acidification in Large Estuaries. *Annual Review of Marine Science*, **13**:23—55. https://doi.org/10.1146/annurev-marine-010419-011004

Casault, B., Johnson, C. L., Devred, E., and Beazley, L. 2025. Chemical and Biological Oceanographic Conditions on the Scotian Shelf and in the Eastern Gulf of Maine during 2023. Can. Tech. Rep. Fish. Aquat. Sci. 3658 : vi + 57 p.

Casey, K. S., Brandon, T.B., Cornillon, P., and Evans, R. 2010. The Past, Present and Future of the AVHRR Pathfinder SST Program. In Oceanography from Space: Revisited. Edited by V. Barale, J.F.R. Gower, and L. Alberotanza. Springer. pp. 273–287.

Chabot, D., & Claireaux, G. 2008. Environmental hypoxia as a metabolic constraint on fish: The case of Atlantic cod, Gadus morhua. Marine Pollution Bulletin. 57: 287–294. https://doi.org/10.1016/j.marpolbul.2008.04.001.

Chabot, D., & Dutil, J.-D. 1999. Reduced growth of Atlantic cod in non-lethal hypoxic conditions. Journal of Fish Biology. 55: 472–491. https://api.semanticscholar.org/CorpusID:84261814.

Chen, C.-T. A., Lui, H.-K., Wang, S.-L. 2017. Deep oceans may acidify faster than anticipated due to global warming. Nature Climate Change. 7: 890–894. https://doi.org/10.1038/nclimate3391.

Chen, C.-T. A., Wang, S.-L. 1999. Carbon, alkalinity and nutrient budgets on the East China Sea continental shelf, Journal of Geophysical Research. 104: 20,675–20,686. https://doi.org/10.1029/1999JC900055.

Claret, M., Galbraith, E. D., Palter, J. B., Bianchi, D., Fennel, K., Gilbert, D., Dunne, J. P. 2018. Rapid coastal deoxygenation due to ocean circulation shift in the northwest Atlantic. Nature Climate Change 8, 868–872. https://doi.org/10.1038/s41558-018-0263-1.

Clements, J. C., & Hunt, H. L. 2017. Effects of CO_2 driven sediment acidification on infaunal marine bivalves: A synthesis. Marine Pollution Bulletin. 117(1–2): 6–16. https://doi.org/10.1016/j.marpolbul.2017.01.053.

Clements, J. C., & Hunt, H. L. 2018. Testing for sediment acidification effects on within-season variability in juvenile soft-shell clam (Mya arenaria) abundance on the northern shore of the Bay of Fundy. Estuaries and Coasts. 41(2): 471–483. https://doi.org/10.1007/s12237-017-0270-x.

CMEMS (Copernicus Marine Service Information). 2025. Global Ocean acidification—mean sea water pH time series and trend from Multi-Observations Reprocessing. E.U. Marine Data Store (MDS). https://doi.org/10.48670/moi-00224 (Accessed on 17-02-2025).

Cyr, F., Bourgault, D. and Galbraith, P. S. 2011. Interior versus boundary mixing of a cold intermediate layer. J. Geophys. Res. (Oceans), 116, C12029, doi:10.1029/2011JC007359

Cyr, F. and Galbraith, P.S. 2021. A climate index for the Newfoundland and Labrador shelf. Earth Syst. Sci. Data, 13, 1807–1828, https://doi.org/10.5194/essd-13-1807-2021, 2021.

Cyr, F., Coyne, J., Snook, S., Bishop, C., Galbraith, P. S., Chen, N., & Han, G. 2024. Physical Oceanographic Conditions on the Newfoundland and Labrador Shelf during 2023. Canadian Technical Report of Hydrography and Ocean Sciences, 382, iv + 54 p.

Cyronak, T., Schulz, K. G., Jokiel, P. L. 2016. The Omega myth: what really drives lower calcification rates in an acidifying ocean. ICES Journal of Marine Science. 73(3): 558–562. https://doi.org/10.1093/icesjms/fsv075.

DFO. 2023. Oceanographic conditions in the Atlantic zone in 2022. Sci. Advis. Sec. Sci. Advis. Rep., 2022/019. ISSN 1919–5087

Diaz, R. J., Rosenberg, R., Sturdivant, K. 2019. Hypoxia in estuaries and semi-enclosed seas. In Ocean Deoxygenation: Everyone's Problem. Causes, Impacts, Consequences and Solutions, D. Laffoley and J.M. Baxter, eds. (IUCN), pp. 85–116.

Dixson, D. L., Jennings, A. R., Atema, J., & Munday, P. L. 2015. Odor Tracking in Sharks Is Reduced under Future Ocean Acidification Conditions. Global Change Biology. 21(4): 1454–1462. https://doi.org/10.1111/gcb.12678.

Dixson, D. L., Munday, P. L., Jones, G. P. 2010. Ocean acidification disrupts the innate ability of fish to detect predator olfactory cues. Ecology Letters .13(1): 68–75. https://doi.org/10.1111/j.1461-0248. 2009.01400.

Doney, S. C. 2010.The Growing Human Footprint on Coastal and Open-Ocean Biogeochemistry. Science, **328**:1512-1516. https://doi.org/10.1126/science.1185198

Doney, S. C., Busch, D. S., Cooley, S. R., & Kroeker, K. J. 2020. The Impacts of Ocean Acidification on Marine Ecosystems and Reliant Human Communities. Annual Review of Environment and Resources. 45: 83–112. https://doi.org/10.1146/annurev-environ-012320-083019.

Falkowski, P. G., Algeo, T., Codispoti, L., Deutsch, C., Emerson, S., Hales, B., Huey, R. B., Jenkins, W. J., Kump, L. R., Levin, L. A., Lyons, T. W., Nelson, N. B., Schofield, O. S., Summons, R., Talley, L. D., Thomas, E., Whitney, F., Pilcher, C. B. 2011. Ocean deoxygenation: Past, present, and future, Eos Trans. AGU. 92(46): 409–410. https://doi.org/10.1029/2011EO460001.

Fassbender, A. J., Carter, B. R., Sharp, J. D., Huang, Y., Arroyo, M. C., Frenzel, H. 2023. Amplified subsurface signals of ocean acidification. Global Biogeochemical Cycles. 37: e2023GB007843. https://doi.org/10.1029/2023GB007843.

Feely, R. A., Alin, S. R., Carter, B., Bednaršek, N., Hales, B., Chan, F., Hill, T. M., Gaylord, B., Sanford, E., Byrne, R. H., Sabine, C. L., Greeley, D., & Juranek, L. 2016. Chemical and biological impacts of ocean acidification along the west coast of North America. Estuarine, Coastal and Shelf Science. 183(Part A): 260–270. https://doi.org/10.1016/j.ecss.2016.08.043.

Feely, R. A., Okazaki, R. R., Cai, W.-J., Bednaršek, N., Alin, S. R., Byrne, R. H., & Fassbender, A. 2018. The combined effects of acidification and hypoxia on pH and aragonite saturation in the coastal waters of the California current ecosystem and the northern Gulf of Mexico. Continental Shelf Research. 152: 50–60. https://doi.org/10.1016/j.csr.2017.11.002.

Fennel, K., Wilkin, J. 2009. Quantifying biological carbon export for the northwest North Atlantic continental shelves. Geophysical Research Letters. 36:L18605. https://doi.org/10.1029/2009GL039818.

Figuerola, B., Hancock, A. M., Bax, N., Cummings, V. J., Downey, R., Griffiths, H. J., Smith, J., & Stark, J. S. 2021. A Review and Meta-Analysis of Potential Impacts of Ocean Acidification on Marine Calcifiers From the Southern Ocean. Frontiers in Marine Science. 8: 584445. https://doi.org/10.3389/fmars.2021.584445.

Friedlingstein, P., O'Sullivan, M., Jones, M. W., Andrew, R. M., Hauck, J., Landschützer, P., Le Quéré, C., Li, H., Luijkx, I. T., Olsen, A., Peters, G. P., Peters, W., Pongratz, J., Schwingshackl, C., Sitch, S., Canadell, J. G., Ciais, P., Jackson, R. B., Alin, S. R., Arneth, A., Arora, V., Bates, N. R., Becker, M., Bellouin, N., Berghoff, C. F., Bittig, H. C., Bopp, L., Cadule, P., Campbell, K., Chamberlain, M. A., Chandra, N., Chevallier, F., Chini, L. P., Colligan, T., Decayeux, J., Djeutchouang, L., Dou, X., Duran Rojas, C., Enyo, K., Evans, W., Fay, A., Feely, R. A., Ford, D. J., Foster, A., Gasser, T., Gehlen, M., Gkritzalis, T., Grassi, G., Gregor, L., Gruber, N., Gürses, Ö., Harris, I., Hefner, M., Heinke, J., Hurtt, G. C., Iida, Y., Ilyina, T., Jacobson, A. R., Jain, A., Jarníková, T., Jersild, A., Jiang, F., Jin, Z., Kato, E., Keeling, R. F., Klein Goldewijk, K., Knauer, J., Korsbakken, J. I., Lauvset, S. K., Lefèvre, N., Liu, Z., Liu, J., Ma, L., Maksyutov, S., Marland, G., Mayot, N., McGuire, P., Metzl, N., Monacci, N. M., Morgan, E. J., Nakaoka, S.-I., Neill, C., Niwa, Y., Nützel, T., Olivier, L., Ono, T., Palmer, P. I., Pierrot, D., Qin, Z., Resplandy, L., Roobaert, A., Rosan, T. M., Rödenbeck, C., Schwinger, J., Smallman, T. L., Smith, S., Sospedra-Alfonso, R., Steinhoff, T., Sun, Q., Sutton, A. J., Séférian, R., Takao, S., Tatebe, H., Tian, H., Tilbrook, B., Torres, O., Tourigny, E., Tsujino, H., Tubiello, F., van der Werf, G., Wanninkhof, R., Wang, X., Yang, D., Yang, X., Yu, Z., Yuan, W., Yue, X., Zaehle, S., Zeng, N., Zeng, J. 2024. Global Carbon Budget 2024. Earth System Science Data Discussions [preprint]. https://doi.org/10.5194/essd-2024-519.

Friedrich, T., Timmermann, A., Abe-Ouchi, A., Bates, N. R., Chikamoto, M. O., Church, M. J., Dore, J. E., Gledhill, D. K., González-Dávila, M., Heinemann, M., Ilyina, T., Jungclaus, J. H., McLeod, E., Mouchet, A., Santana-Casiano, J. M. 2012. Detecting regional anthropogenic trends in ocean acidification against natural variability. Nature Climate Change. 2(3): 167–171. https://doi.org/10.1038/nclimate1372.

Galbraith, P. S., 2006. Winter water masses in the Gulf of St. Lawrence. J. Geophys. Res. (Oceans), 111, C06022. doi: 10.1029/2005JC003159

Galbraith, P. S. and P. Larouche. 2013. Trends and variability in eastern Canada sea-surface temperatures. Ch.1 In: Aspects of climate change in the Northwest Atlantic off Canada [Loder, J. W., G. Han, P. S. Galbraith, J. Chassé and A. van der Baaren (Eds.)]. Can. Tech. Rep. Fish. Aquat. Sci. 3045: x + 192 p.

Galbraith, P.S., Chassé, J., Caverhill, C., Nicot, P., Gilbert, D., Pettigrew, B., Lefaivre, D., Brickman, D., Devine, L., and Lafleur, C. 2017. Physical Oceanographic Conditions in the Gulf of St. Lawrence in 2016. DFO Can. Sci. Advis. Sec. Res. Doc. 2017/044. v + 91 p.

Galbraith, P. S., Larouche, P., Caverhill. C. 2021. A sea-surface temperature homogenization blend for the Northwest Atlantic. Can. J. Remote Sensing. **47**(4): 554–568DOI: 10.1080/07038992.2021.1924645

Galbraith, P. S., Chassé, J., Shaw, J.-L., Dumas, J. and Bourassa, M.-N. 2024a. Physical Oceanographic Conditions in the Gulf of St. Lawrence during 2023. Can. Tech. Rep. Hydrogr. Ocean Sci. 378 : v + 91 p

Galbraith, P. S., C. Sévigny, D. Bourgault and D. Dumont. 2024b. Sea ice interannual variability and sensitivity to fall oceanic conditions and winter air temperature in the Gulf of St. Lawrence, Canada. J. Geophys. Res. Oceans, 129:7, e2023JC020784. https://doi.org/10.1029/2023JC020784

Galbraith, P. S., Chassé, J., Shaw, J.-L., Lefaivre, D. and Bourassa, M.-N. 2025. Physical Oceanographic Conditions in the Gulf of St. Lawrence during 2024. Can. Tech. Rep. Hydrogr. Ocean Sci. 397: v + 95 p.

Gattuso, J.-P., Hansson. L. (eds). 2020. Ocean Acidification. Oxford Academic. https://doi.org/10.1093/oso/9780199591091.001.0001.

Gazeau, F., Parker, L. M., Comeau, S., Gattuso, J.-P., O'Connor, W. A., Martin, S., Pörtner, H.-O., Ross, P. M. 2013. Impacts of ocean acidification on marine shelled molluscs. Marine Biology. 160(8): 2207–2245. https://doi.org/10.1007/s00227-013-2219-3.

Gibb, O., Cyr, F., Azetsu-Scott, K., Chassé, J., Childs, D., Gabriel, C.-E., Galbraith, P. S., Maillet, G., Pepin, P., Punshon, S., and Starr, M. 2023. Spatiotemporal variability in pH and carbonate parameters on the Canadian Atlantic continental shelf between 2014 and 2022. Earth Syst. Sci. Data, **15**: 4127–4162, https://doi.org/10.5194/essd-15-4127-2023.

Gilbert, D. 2004. Propagation of temperature signals from the northwest Atlantic continental shelf edge into the Laurentian Channel. ICES CM. 2004/N: 7. 12 p.

Gilbert, D. and Pettigrew, B. 1997. Interannual variability (1948–1994) of the CIL core temperature in the Gulf of St. Lawrence. Can. J. Fish. Aquat. Sci., 54 (Suppl. 1), 57–67.

Gilbert, D., Sundby, B., Gobeil, C., Mucci, A., & Tremblay, G.-H. 2005. A seventy-two-year record of diminishing deep-water oxygen in the St. Lawrence estuary: The northwest Atlantic connection. Limnology and Oceanography, **50**(5): 1654–1666. https://doi.org/10.4319/lo.2005.50.5.1654

Gilbert, D., Rabalais, N. N., Díaz, R. J., and Zhang, J. 2010. Evidence for greater oxygen decline rates in the coastal ocean than in the open ocean. Biogeosciences. 7: 2283–2296. https://doi.org/10.5194/bg-7-2283-2010.

Gobler, C. J., Baumann, H. 2016. Hypoxia and acidification in ocean ecosystems: coupled dynamics and effects on marine life. Biology Letters. 12(5): 20150976. https://doi.org/10.1098/rsbl.2015.0976.

Gruber, N., Bakker, D. C. E., DeVries, T., Gregor, L., Hauck, J., Landschützer, P., McKinley, G. A., Müller, J. D. 2023. Trends and variability in the ocean carbon sink. Nature Reviews Earth & Environment. 4(2): 119–134. https://doi.org/10.1038/s43017-022-00381-x.

Gruber, N., Clement, D., Carter, B. R., Feely, R. A., van Heuven, S., Hoppema, M., Ishii, M., Key, R. M., Kozyr, A., Lauvset, S. K., Lo Monaco, C., Mathis, J. T., Murata, A., Olsen, A., Pérez, F. F., Sabine, C. L., Tanhua, T., Wanninkhof, R. 2019. The oceanic sink for anthropogenic CO_2 from 1994 to 2007. Science. 363(6432): 1193–1199. https://doi.org/10.1126/science.aau5153.

Han, G., Chen, N., & Ma, Z. 2014. Is there a north-south phase shift in the surface Labrador Current transport on the interannual-to-decadal scale? Journal of Geophysical Research: Oceans, **119**(1): 276–287. https://doi.org/10.1002/2013JC009102

Hebert, D., Layton, C., Brickman, D., and Galbraith, P.S. 2024. Physical Oceanographic Conditions on the Scotian Shelf and in the Gulf of Maine during 2023. Can. Tech. Rep. Hydrogr. Ocean Sci. 380: vi + 71 p.

Heuer, R. M., Grosell, M. 2014. Physiological impacts of elevated carbon dioxide and ocean acidification on fish. AJP Regulatory Integrative and Comparative Physiology. 307(9): R1061-R1084. https://doi.org/10.1152/ajpregu.00064.2014.

Heuer, R. M., Grosell, M. 2014. Physiological impacts of elevated carbon dioxide and ocean acidification on fish. AJP Regulatory Integrative and Comparative Physiology. 307(9): R1061-R1084. https://doi.org/10.1152/ajpregu.00064.2014.

IPBES. 2019. Summary for policymakers of the global assessment report on biodiversity and ecosystem services of the Intergovernmental Science-Policy Platform on Biodiversity and Ecosystem Services. In: Global assessment report on biodiversity and ecosystem services of the Intergovernmental Science-Policy Platform on Biodiversity and Ecosystem Services [Díaz, S., J. Settele, E.S. Brondízio, H.T. Ngo, M. Guèze, J. Agard, A. Arneth, P. Balvanera, K.A. Brauman, S.H.M. Butchart, K.M.A. Chan, L.A. Garibaldi, K. Ichii, J. Liu, S.M. Subramanian, G.F. Midgley, P. Miloslavich, Z. Molnár, D. Obura, A. Pfaff, S. Polasky, A. Purvis, J. Razzaque, B. Reyers, R.R. Chowdhury, Y.J. Shin, I.J. Visseren-Hamakers, K.J. Willis, and C.N. Zayas (eds.)]. Intergovernmental Science-Policy Platform on Biodiversity and Ecosystem Services (IPBES) Secretariat, Bonn, Germany, pp. 56. https:// doi.org/10.5281/zenodo.3553579.

IPCC. 2021. Climate Change 2021: The Physical Science Basis. Contribution of Working Group I to the Sixth Assessment Report of the Intergovernmental Panel on Climate Change [Masson-Delmotte, V., P. Zhai, A. Pirani, S.L. Connors, C. Péan, S. Berger, N. Caud, Y. Chen, L. Goldfarb, M.I. Gomis, M. Huang, K. Leitzell, E. Lonnoy, J.B.R. Matthews, T.K. Maycock, T. Waterfield, O. Yelekçi, R. Yu, and B. Zhou (eds.)]. Cambridge University Press, Cambridge, United Kingdom and New York, NY, USA, 2391 pp. https://doi.org/10.1017/9781009157896.

Jiang, L. Q., Carter, B. R., Feely, R. A., Lauvset, S. K., Olsen, A. 2019. Surface ocean pH and buffer capacity: past, present and future. Scientific Reports. 9: 18624. https://doi.org/10.1038/s41598-019-55039-4.

Jokiel, P. L. 2011. Ocean acidification and control of reef coral calcification by boundary layer limitation of proton flux. Bulletin of Marine Science. 87(3): 639–657. https://doi.org/10.5343/bms.2010.1107.

Jokiel, P. L. 2013. Coral reef calcification: carbonate, bicarbonate and proton flux under conditions of increasing ocean acidification. Proceedings of the Royal Society B: Biological Sciences. 280(1769): 20130031. https://doi.org/10.1098/rspb.2013.0031.

Jonasson, O.; Gladkova, I.; Ignatov, A. Towards global daily gridded super-collated SST product from low earth orbiting satellites (L3S-LEO-Daily) at NOAA. Proc. SPIE 2022, 12118, 1211805, doi:10.1117/12.2620103

Jutras, M., Dufour, C. O., Mucci, A., Cyr, F., Gilbert, D. 2020. Temporal changes in the causes of the observed oxygen decline in the St. Lawrence Estuary. Journal of Geophysical Research: Oceans, 125, e2020JC016577. https://doi.org/10.1029/2020JC016577

Jutras, M., Dufour, C. O., Mucci, A., Talbot, L. C. 2023a. Large-scale control of the retroflection of the Labrador Current. Nature Communications 14:2623. https://doi.org/10.1038/s41467-023-38321-y

Jutras, M., Mucci, A., Chaillou, G., Nesbitt, W. A., Wallace, D. W. R. 2023b. Temporal and spatial evolution of bottom-water hypoxia in the St Lawrence estuarine system. Biogeosciences, 20, 839–849, 2023. https://doi.org/10.5194/bg-20-839-2023

Kahil, K., Weiner, S., Addadi, L., & Gal, A. 2021. Ion pathways in biomineralization: Perspectives on uptake, transport, and deposition of calcium, carbonate, and phosphate. Journal of the American Chemical Society. 143(50): 21100–21112. https://doi.org/10.1021/jacs.1c09174.

Keeling, R. F., Körtzinger , A., Gruber, N. 2010. Ocean Deoxygenation in a Warming World. Annual Review of Marine Science. 2:199-229. https://doi.org/10.1146/annurev.marine.010908.163855.

Keppel, E. A., Scrosati, R. A., Courtenay, S. C. 2012. Ocean acidification decreases growth and development in American lobster (Homarus americanus) larvae. Journal of Northwest Atlantic Fishery Science. 44: 61–66. https://doi.org/10.2960/J.v44.m683.

Kroeker, K. J., Kordas, R. L., Crim, R. N., & Singh, G. G. 2010. Meta-analysis reveals negative yet variable effects of ocean acidification on marine organisms. Ecology Letters. 13(11): 1419-1434. https://doi.org/10.1111/j.1461-0248.2010.01518.x.

Kroeker, K. J., Kordas, R. L., Crim, R., Hendriks, I. E., Ramajo, L., Singh, G. S., Duarte, C. M., & Gattuso, J. P. 2013. Impacts of ocean acidification on marine organisms: quantifying sensitivities and interaction with warming. Global Change Biology. 19(6): 1884–1896. https://doi.org/10.1111/gcb.12179.

Larouche, P. and P. S. Galbraith. 2016. Canadian coastal seas and Great Lakes sea surface temperature climatology and recent trends. Canadian Journal of Remote Sensing, 42:3, 243–258, DOI: 10.1080/07038992.2016.1166041

Lauvset, S. K., Carter, B. R., Pérez, F. F., Jiang, L.-Q., Feely, R. A., Velo, A., Olsen, A. 2020. Processes driving global interior ocean pH distribution. Global Biogeochemical Cycles. 34: e2019GB006229. https://doi.org/10.1029/2019GB006229.

Lavoie, D., Lambert, N., Rousseau, S., Dumas, J., Chassé, J., Long, Z., Perrie, W., Starr, M., Brickman, D., Azetsu-Scott, K. 2020. Projections of future physical and biochemical conditions in the Gulf of St. Lawrence, on the Scotian Shelf and in the Gulf of Maine using a regional climate model. Can. Tech. Rep. Hydrogr. Ocean Sci. 334: xiii + 102 p.

Lee, C.-H., Lee, K., Lee, J.-S., Jeong, K.-Y., Ko, Y.-H. 2024. Persistent organic alkalinity in the ocean. Geochimica et Cosmochimica Acta. 387: 53–62. https://doi.org/10.1016/j.gca.2024.06.010.

Lee, K., Sabine, C. L., Tanhua, T., Kim, T.-W., Feely, R. A., Kim, H.-C. 2011. Roles of marginal seas in absorbing and storing fossil fuel CO_2. Energy and Environmental Science. 4(4): 1133–1146. https://doi.org/10.1039/C0EE00663G.

Leung, J. Y. S., Zhang, S., & Connell, S. D. 2022. Is Ocean Acidification Really a Threat to Marine Calcifiers? A Systematic Review and Meta-Analysis of 980+ Studies Spanning Two Decades. Small. 18(35): 2107407. https://doi.org/10.1002/smll.202107407.

Levin, L. A. 2018. Manifestation, drivers, and emergence of open ocean deoxygenation. Annual Review in Marine Science. 10: 229–260. https://doi.org/10.1146/annurev-marine-121916-063359.

Limburg, K. E., Breitburg, D., Swaney, D. P., & Jacinto, G. 2020. Ocean Deoxygenation: A Primer. One Earth. 2(1): 24–29. https://doi.org/10.1016/j.oneear.2020.01.001.

Long, W. C., Swiney, K. M., Foy, R. J. 2016. Effects of high pCO_2 on Tanner crab reproduction and early life history, Part II: Carryover effects on larvae from oogenesis and embryogenesis are stronger than direct effects. ICES Journal of Marine Science. 73(3): 836–848. https://doi.org/10.1093/icesjms/fsv251.

Mackinder, L., Wheeler, G., Schroeder, D., Riebesell, U., & Brownlee, C. 2010. Molecular mechanisms underlying calcification in coccolithophores. Geomicrobiology Journal. 27(6–7): 585–595. https://doi.org/10.1080/01490451003703014.

Mann, S. 2001. Biomineralization: principles and concepts in bioinorganic materials chemistry. Oxford University Press, New York. 1–205.

McNeil, B. I., Sasse, T. P. 2016. Future ocean hypercapnia driven by anthropogenic amplification of the natural CO2 cycle. Nature. 529(7586): 383–386. https://doi.org/10.1038/nature16156.

Michaelidis, B., Ouzounis, C., Paleras, A., Pörtner, H. O. 2005. Effects of long-term moderate hypercapnia on acid-base balance and growth rate in marine mussels Mytilus gallo provincialis. Marine Ecology Progress Series. 293: 109–118. https://api.semanticscholar.org/CorpusID:38976796.

Mitchell, M. R., Harrison, G., Pauley, K., Gagné, A., Maillet, G., and Strain, P. 2002. Atlantic Zonal Monitoring Program sampling protocol. Can. Tech. Rep. Hydrogr. Ocean Sci. 223: iv + 23 pp.

Millero, F. J., Lee, K., Roche, M. 1998. Distribution of alkalinity in the surface waters of the major oceans. Marine Chemistry. 60(1–2): 111–130. https://doi.org/10.1016/S0304-4203(97)00084-4.

Morse, J. W., Arvidson, R. S., Lüttge, A. 2007. Calcium carbonate formation and dissolution. Chemical Reviews. 107(2): 342–381. https://doi.org/10.1021/cr050358j.

Mucci, A., Starr, M., Gilbert, D., and Sundby, B. 2011. Acidification of Lower St. Lawrence Estuary Bottom Waters. *Atmosphere-Ocean*, **49**(3): 206–218, DOI: 10.1080/07055900.2011.59926

Müller J. D., Gruber, N. 2024. Progression of ocean interior acidification over the industrial era. Science Advances. 10(48): eado3103. https://doi.org/10.1126/sciadv.ado3103.

Munday, P. L., Dixson, D. L., Donelson, J. M., Jones, G. P., Pratchett, M. S., Devitsina, G. V., Døving, K. B. 2009. Ocean acidification impairs olfactory discrimination and homing ability of a marine fish. Proceedings of the National Academy of Sciences of the United States of America. 106(6): 1848–1852. https://doi.org/10.1073/pnas.0809996106.

Nilsson, G. E., Dixson, D. L., Domenici, P., McCormick, M. I., Sørensen, C., Watson, S.-A., Munday, P. L. 2012. Near-future carbon dioxide levels alter fish behaviour by interfering with neurotransmitter function. Nature Climate Change. 2: 201–204. https://doi.org/10.1038/nclimate1352.

Ninokawa, A. T., Saley, A. M., Shalchi, R., Gaylord, B. 2024. Multiple carbonate system parameters independently govern shell formation in a marine mussel. Communications Earth & Environment. 5, 273. https://doi.org/10.1038/s43247-024-01440-5.

NOAA/STAR. 2021. GHRSST NOAA/STAR ACSPO v2.80 0.02 degree L3S Dataset from Afternoon LEO Satellites (GDS v2). Ver. v2.80. PO.DAAC, CA, USA. Geosci. **11**, 467–473. https://doi.org/10.1038/s41561-018-0152-2

Orr, J. C., Fabry, V. J., Aumont, O., Bopp, L., Doney, S. C., Feely, R. A., Gnanadesikan, A., Gruber, N., Ishida, A., Joos, F., Key, R. M., Lindsay, K., Maier-Reimer, E., Matear, R., Monfray, P., Mouchet, A., Najjar, R. G., Plattner, G. K., Rodgers, K. B., Sabine, C. L., Sarmiento, J. L., Schlitzer, R., Slater, R. D., Totterdell, I. J., Weirig, M. F., Yamanaka, Y., Yool, A. 2005. Anthropogenic ocean acidification over the twenty-first century and its impact on calcifying organisms. Nature. 437(7059): 681–686. https://doi.org/10.1038/nature04095.

Orr J. C., Epitalon J.-M. and Gattuso J.-P. 2015. Comparison of seven packages that compute ocean carbonate chemistry. Biogeosciences. 12(5): 1483–1510. https://doi.org/10.5194/bg-12-1483-2015[1].

Oschlies, A., Brandt, P., Stramma, L. et al. 2018. Drivers and mechanisms of ocean deoxygenation. Nature Geosci **11**: 467–473. https://doi.org/10.1038/s41561-018-0152-2

Perry, S. F., Gilmour, K. M. 2006. Acid-base balance and CO_2 excretion in fish: Unanswered questions and emerging models. Respiratory Physiology & Neurobiology. 154(1–2): 199-215. https://doi.org/10.1016/j.resp.2006.04.010.

Pimentel, M. S., Faleiro, F., Marques, T., Bispo, R., Dionisio, G., Faria, A. M., Machado, J., Peck, M. A., Pörtner, H., Pousão-Ferreira, P., Gonçalves, E. J., & Rosa, R. 2016. Foraging behaviour, swimming performance and malformations of early stages of commercially important fishes under ocean acidification and warming. Climatic Change. 137(3), 495–509. https://doi.org/10.1007/s10584-016-1682-5.

Plante, S., Chabot, D., & Dutil, J.-D. 1998. Hypoxia tolerance in Atlantic cod. Journal of Fish Biology. 53: 1342–1356.

Pousse, E., Poach, M. E., Redman, D. H., Sennefelder, G., White, L. E., Lindsey, J. M., Munroe, D., Hart, D., Hennen, D., Dixon, M. S., Li, Y., Wikfors, G. H., & Meseck, S. L. 2020. Energetic response of Atlantic surfclam Spisula solidissima to ocean acidification. Marine Pollution Bulletin. 161: 111740. https://doi.org/10.1016/j.marpolbul.2020.111740.

Pörtner, H.-O., Roberts, D. C., Masson-Delmotte, V., Zhai, P., Tignor, M., Poloczanska, E., Mintenbeck, K., Nicolai, M., Okem, A., Petzold, J., et al. 2019. IPCC special report on the ocean and cryosphere in a changing climate. IPCC Intergovernmental Panel on Climate Change (IPCC).

Rabalais, N. N. 2019. Ocean deoxygenation from eutrophication (human nutrient inputs). In Ocean Deoxygenation: Everyone's Problem. Causes, Impacts, Consequences and Solutions, D. Laffoley and J.M. Baxter, eds. (IUCN), pp. 117–135.

Rheuban, J. E., Doney, S. C., Cooley, S. R., Hart, D. R. 2018. Projected impacts of future climate change, ocean acidification, and management on the US Atlantic sea scallop (Placopecten magellanicus) fishery. PLoS One. 13(9): e0203536. https://doi.org/10.1371/journal.pone.0203536.

Ringuette, M. Devred, E., Azetsu-Scott, K., Head, E., Punshon, S., Casault, B. and Clay, S. 2022. Optical, Chemical, and Biological Oceanographic Conditions in the Labrador Sea between 2014 and 2018. DFO Can. Sci. Advis. Sec. Res. Doc. 2022/021. v + 38 p.

Rodriguez-Dominguez, A., Connell, S. D., Baziret, C., Nagelkerken, I. 2018. Irreversible behavioural impairment of fish starts early: Embryonic exposure to ocean acidification. Marine Pollution Bulletin. 133: 562–567. https://doi.org/10.1016/j. marpolbul.2018.06.004.

Roleda, M. Y., Boyd, P. W., Hurd, C. L. 2012. Before ocean acidification: calcifier chemistry lessons. Journal of Phycology. 48(4): 840-843. https://doi.org/10.1111/j.1529-8817.2012.01195.x.

Roman, M. R., Altieri, A. H., Breitburg, D., Ferrer, E. M., Gallo, N. D., Ito, S., Limburg, K., Rose, K., Yasuhara, M., & Levin, L. A. 2024. Reviews and syntheses: Biological indicators of low-oxygen stress in marine water-breathing animals. Biogeosciences. 21(11): 4975–4995. https://doi.org/10.5194/bg-21-4975-2024.

Rousseau, S., Lavoie, D., Jutras, M., Chassé, J. 2025. Transit time of deep and intermediate waters in the Gulf of St. Lawrence. Ocean Modelling 195, June 2025, 102526.

Sathyendranath, S., Brewin, R. J. W., Brockmann, C., Brotas, V., Calton, B., Chuprin, A., Cipollini, P., Couto, A. B., Dingle, J., Doerffer, R., Donlon, C., Dowell, M., Farman, A., Grant, M., Groom, S., Horseman, A., Jackson, T., Krasemann, H., Lavender, S., Martinez-Vicente, V., … Platt, T. (2019). An Ocean-Colour Time Series for Use in Climate Studies: The Experience of the Ocean-Colour Climate Change Initiative (OC-CCI). Sensors (Basel, Switzerland), 19(19), 4285. https://doi.org/10.3390/s19194285

Schmidtko, S., Stramma, L., Visbeck, M. 2017. Decline in global oceanic oxygen content during the past five decades. Nature 542, 335–339. https://doi.org/10.1038/nature21399.

Siedlecki, S. A., Salisbury, J., Gledhill, D. K., Bastidas, C., Meseck, S., McGarry, K., Hunt, C. W., Alexander, M., Lavoie, D., Wang, Z. A., Scott, J., Brady, D. C., Mlsna, I., Azetsu-Scott, K., Liberti, C. M., Melrose, D. C., White, M. M., Pershing, A., Vandemark, D., Townsend, D. W., Chen, C., Mook, W., Morrison, R. 2021. Projecting ocean acidification impacts for the Gulf of Maine to 2050: New tools and expectations. Elementa: Science of the Anthropocene 9(1). https://doi.org/10.1525/elementa.2020.00062.

Stevens, S.W., Pawlowicz, R., Tanhua, T., Gerke, L., Nesbitt, W.A., Drozdowski, A., Chassé, J., Wallace, D.W.R. 2024. Deep inflow transport and dispersion in the Gulf of St. Lawrence revealed by a tracer release experiment. *Commun Earth Environ* **5**, 338 (2024). https://doi.org/10.1038/s43247-024-01505-5

Stumpp, M., Hu, M. Y., Melzner, F., Gutowska, M. A., Dorey, N., Himmerkus, N., Holtmann, W. C., Dupont, S. T., Thorndyke, M. C., & Bleich, M. 2012. Acidified seawater impacts sea urchin larvae pH regulatory systems relevant for calcification. Proceedings of the National Academy of Sciences, 109(44), 18192–18197. https://doi.org/10.1073/pnas.1209174109.

Therriault, J.-C., Petrie, B., Pepin, P., Gagnon, J., Gregory, D., Helbig, J., Herman, A., Lefaivre, D., Mitchell, M., Pelchat, B., Runge, J., and Sameoto, D. 1998. Proposal for a northwest Atlantic zonal monitoring program. Can. Tech. Rep. Hydrogr. Ocean Sci. 194: vii+57p.

Thomsen, J., Haynert, K., Wegner, K. M., Melzner, F. 2015. Impact of seawater carbonate chemistry on the calcification of marine bivalves. Biogeosciences. 12(14) : 4209–4220. https://doi.org/10.5194/bg-12-4209-2015.

Toyofuku, T., Matsuo, M., de Nooijer, L. J., Nagai, Y., Kawada, S., Fujita, K., Reichart, G.-J., Nomaki, H., Tsuchiya, M., Sakaguchi, H., Kitazato, H. 2017. Proton pumping accompanies calcification in foraminifera. Nature Communications. 8: 14145. https://doi.org/10.1038/ncomms14145.

Umoh, J. U. and Thompson, K. R. 1994. Surface heat flux, horizontal advection, and the seasonal evolution of water temperature on the Scotian Shelf. J. Geophys. Res., 99, 20403–20416.

Umoh, J. U., Loder, J. W., and Petrie, B. 1995. The role of air sea heat fluxes in annual and interannual ocean temperature variability on the eastern Newfoundland Shelf. Atmos.-Ocean, 33(3), 531–568.

Vaquer-Sunyer, R., & Duarte, C. M. 2008. Thresholds of hypoxia for marine biodiversity. Proceedings of the National Academy of Sciences of the United States of America. 105(40): 15452–15457. https://doi.org/10.1073/pnas.0803833105.

Waldbusser, G. G., & Salisbury, J. E. 2014. Ocean acidification in the coastal zone from an organism's perspective: Multiple system parameters, frequency domains, and habitats. Annual Review of Marine Science. 6(1): 221–247. https://doi.org/10.1146/annurev-marine-121211-172238.

Wang, Z. A., Cai, W.-J. 2004. Carbon dioxide degassing and inorganic carbon export from a marsh-dominated estuary (the Duplin River): A marsh CO_2 pump. Limnology and Oceanography. 49: 341–354. https://doi.org/10.4319/lo.2004.49.2.0341

Weiss, R. 1974. Carbon Dioxide in Water and Seawater: The Solubility of a Non-Ideal Gas. Marine Chemistry. 2: 203–215. http://dx.doi.org/10.1016/0304-4203(74)90015-2.

Woods, H. A., Moran, A. L., Atkinson, D., Audzijonyte, A., Berenbrink, M., Borges, F. O., Burnett, K. G., Burnett, L. E., Coates, C. J., Collin, R., Costa-Paiva, E. M., Duncan, M. I., Ern, R., Laetz, E. M. J., Levin, L. A., Lindmark, M., Lucey, N. M., McCormick, L. R., Pierson, J. J., Rosa, R., Roman, M. R., Sampaio, E., Schulte, P. M., Sperling, E. A., Walczynska, A., Verberk, W. C. E. P. 2022. Integrative approaches to understanding organismal responses to aquatic deoxygenation. Biology Bulletin. 243, 85–103. https://doi.org/10.108.6/722899.

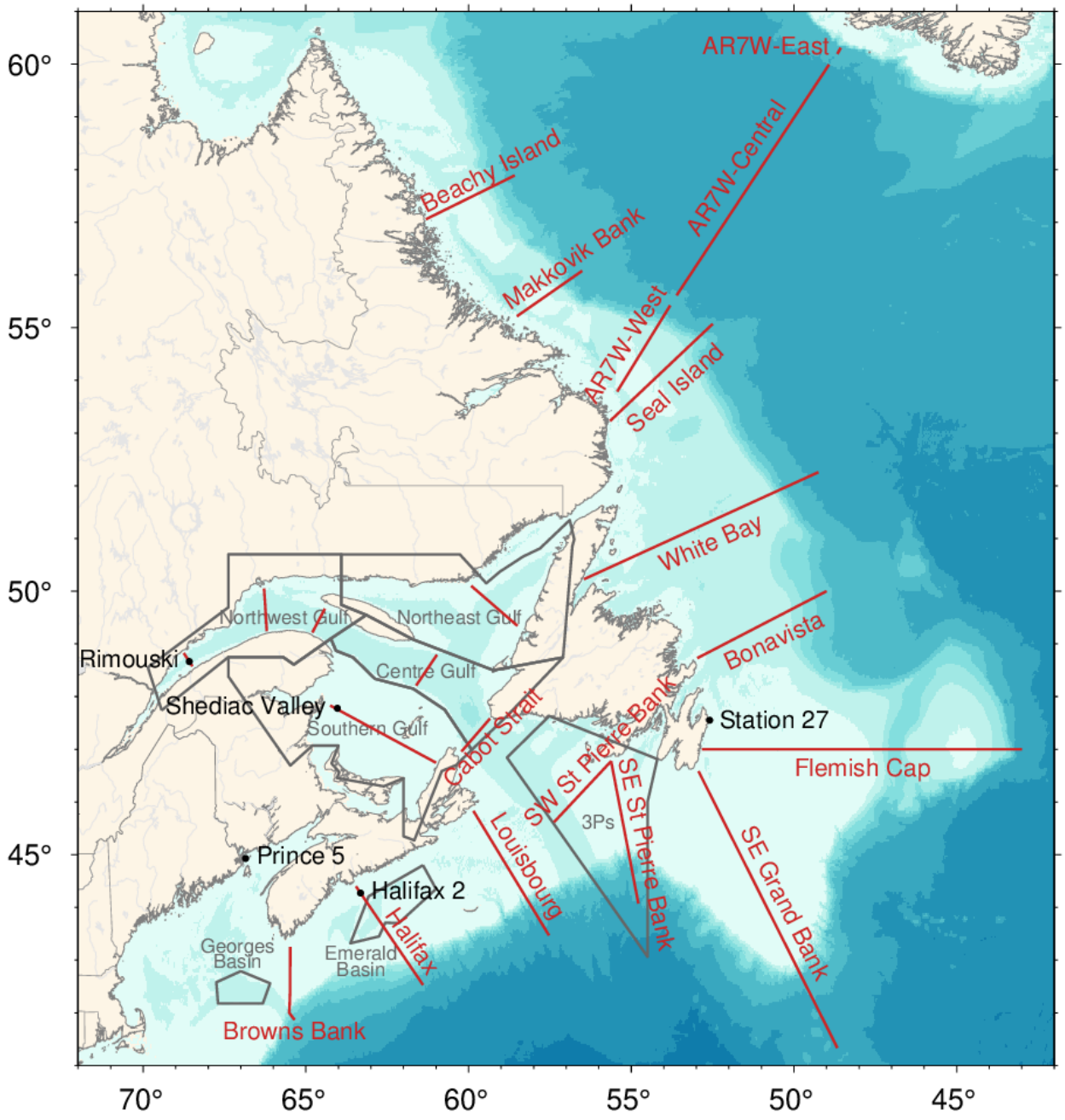

Figure 1. Atlantic Zone Monitoring Program high-frequency sampling stations (black), selected section lines (red) and averaging areas (gray).

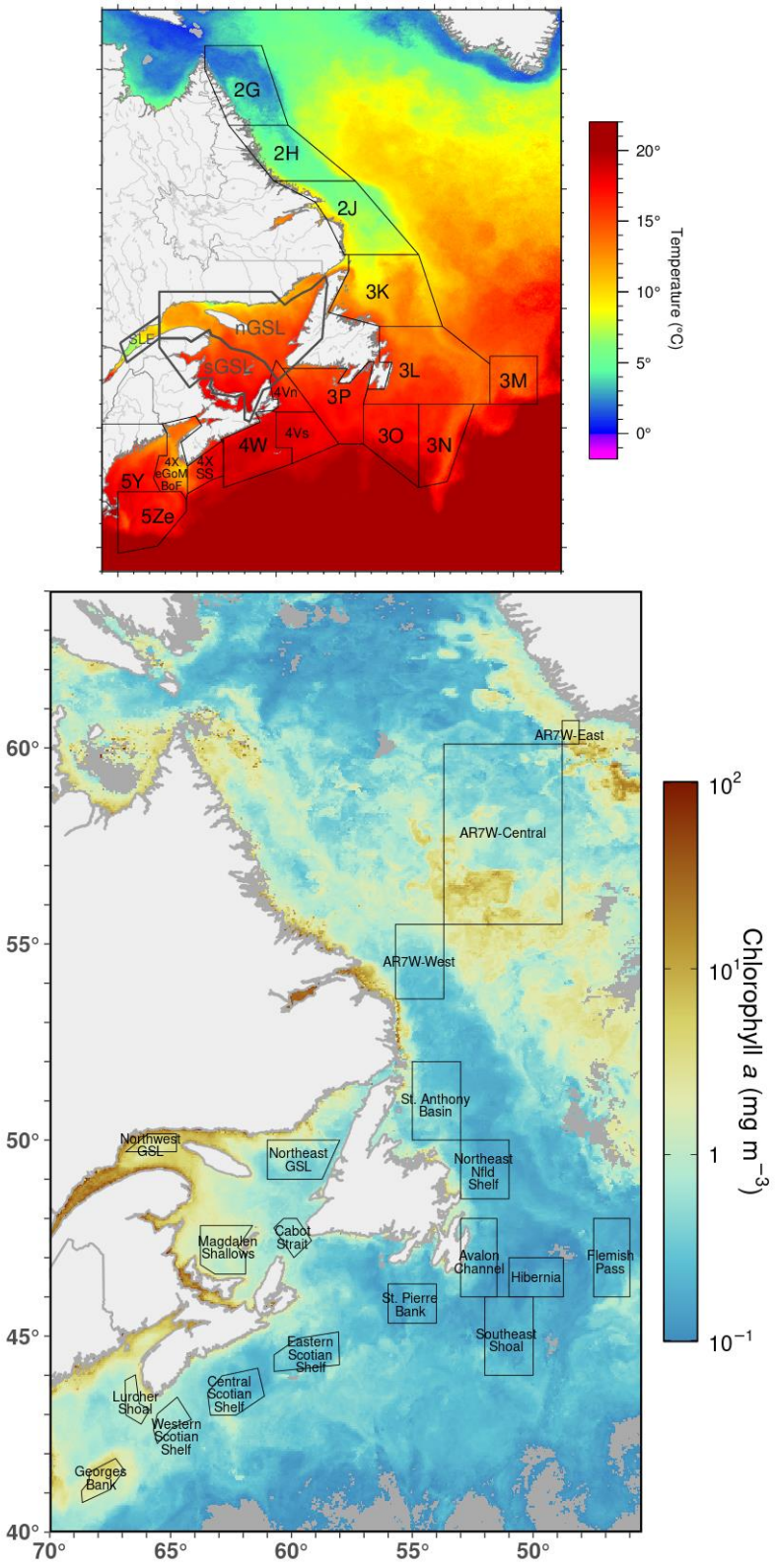

Figure 2. Areas used for (top) temperature and (bottom) ocean colour averages. (Top) North Atlantic Fisheries Organization Divisions are cut off at the shelf break. The acronyms GSL and SLE are Gulf of St. Lawrence and St. Lawrence Estuary respectively. Sea surface temperatures are shown for September 2024 and ocean colour chlorophyll *a* concentrations are for June 2024.

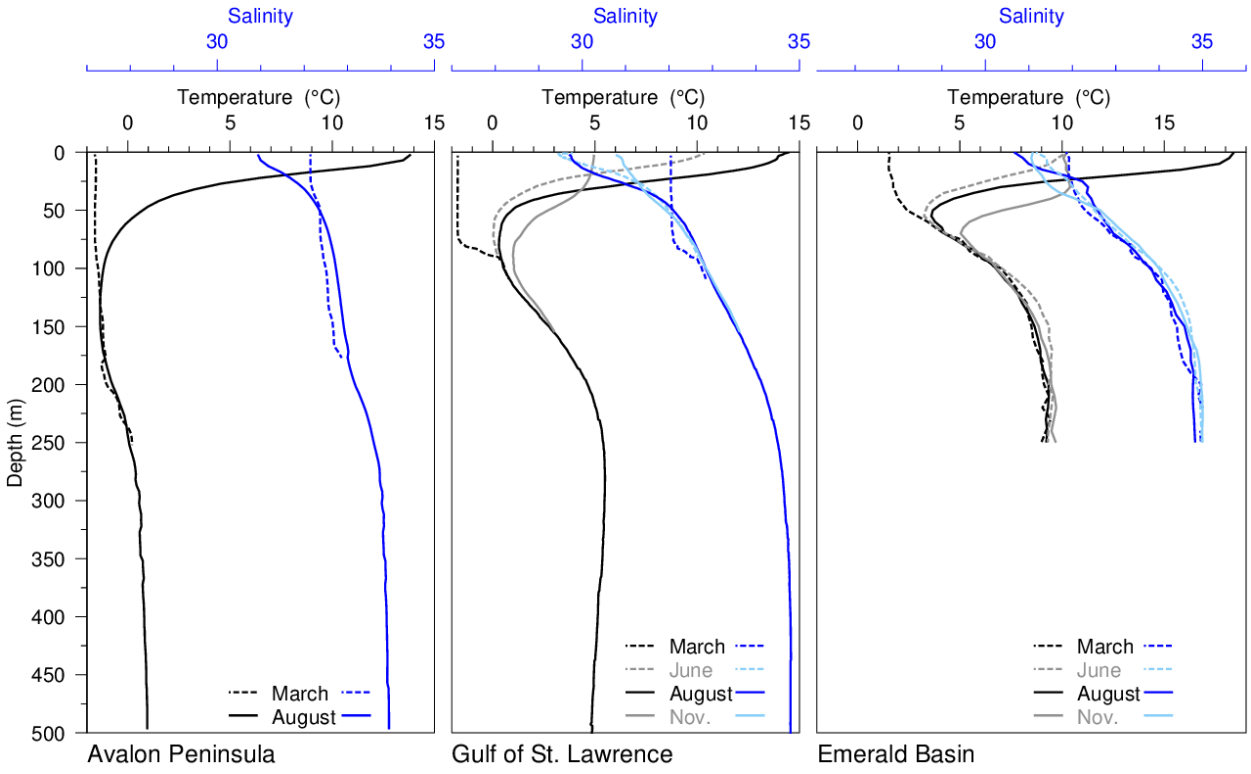

Figure 3. Typical seasonal progression of the depth profile of temperature and salinity observed in three representative regions across the zone. The Avalon Peninsula region is delimited by 45–50°N and 50–55°W and shown are the averages of profiles for March and August between 2015 and 2017, calculated from 5 and 302 profiles respectively. The Gulf of St. Lawrence profiles are averages of observations in June, August and November 2007 in the northern Gulf, while the March profile shows a single winter temperature profile (March 2008), with near-freezing temperatures in the top 75 m. The Emerald Basin profiles are monthly climatological averages for 1981–2010.

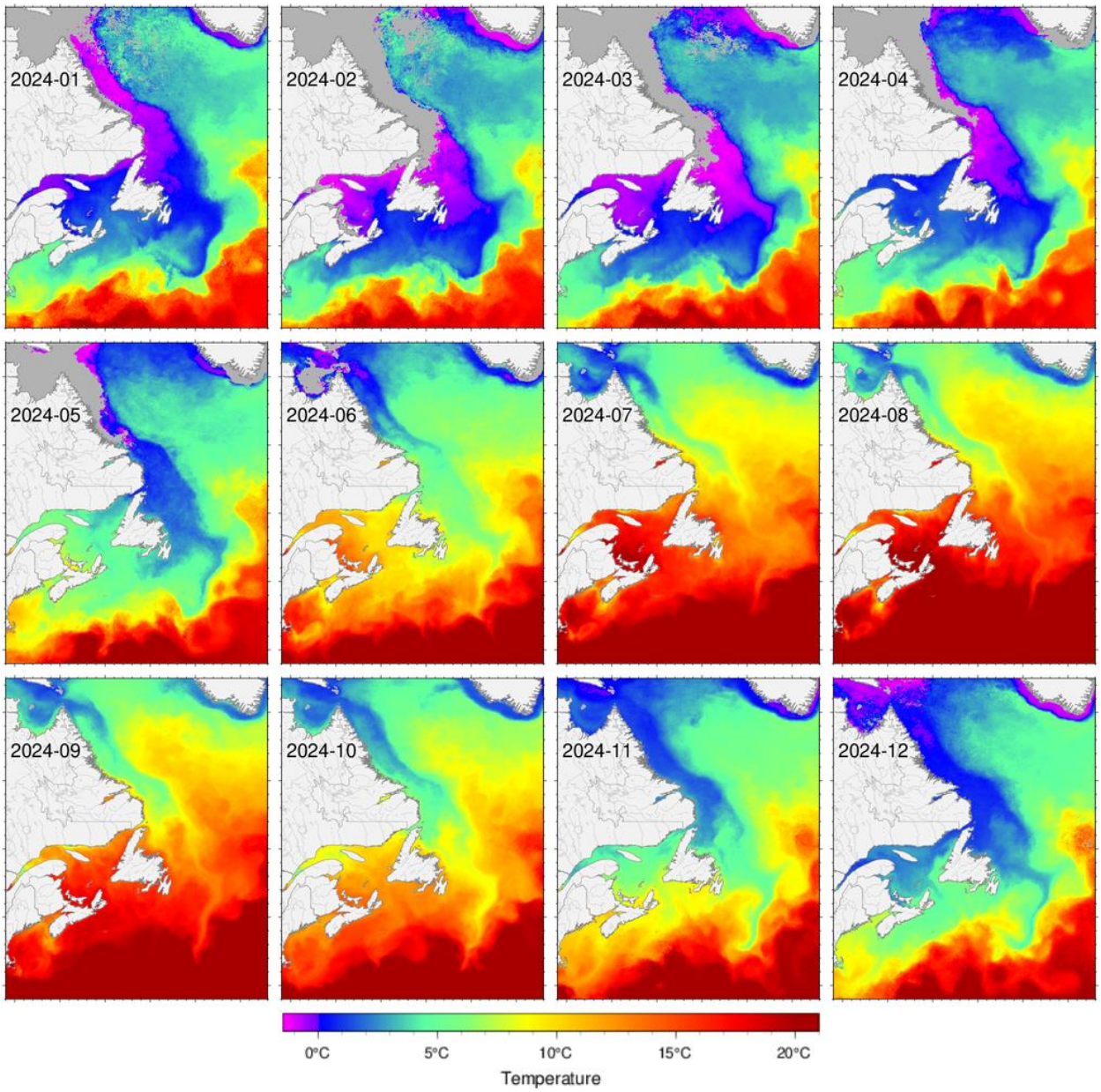

Figure 4. Sea surface temperature monthly averages for 2024 in the Atlantic zone. Grey areas have no data for the period due to ice cover or clouds. Temperatures are biased towards warmer ice-free conditions for all months affected by sea ice cover, as the freezing conditions of the ice-covered areas are not captured by satellite.

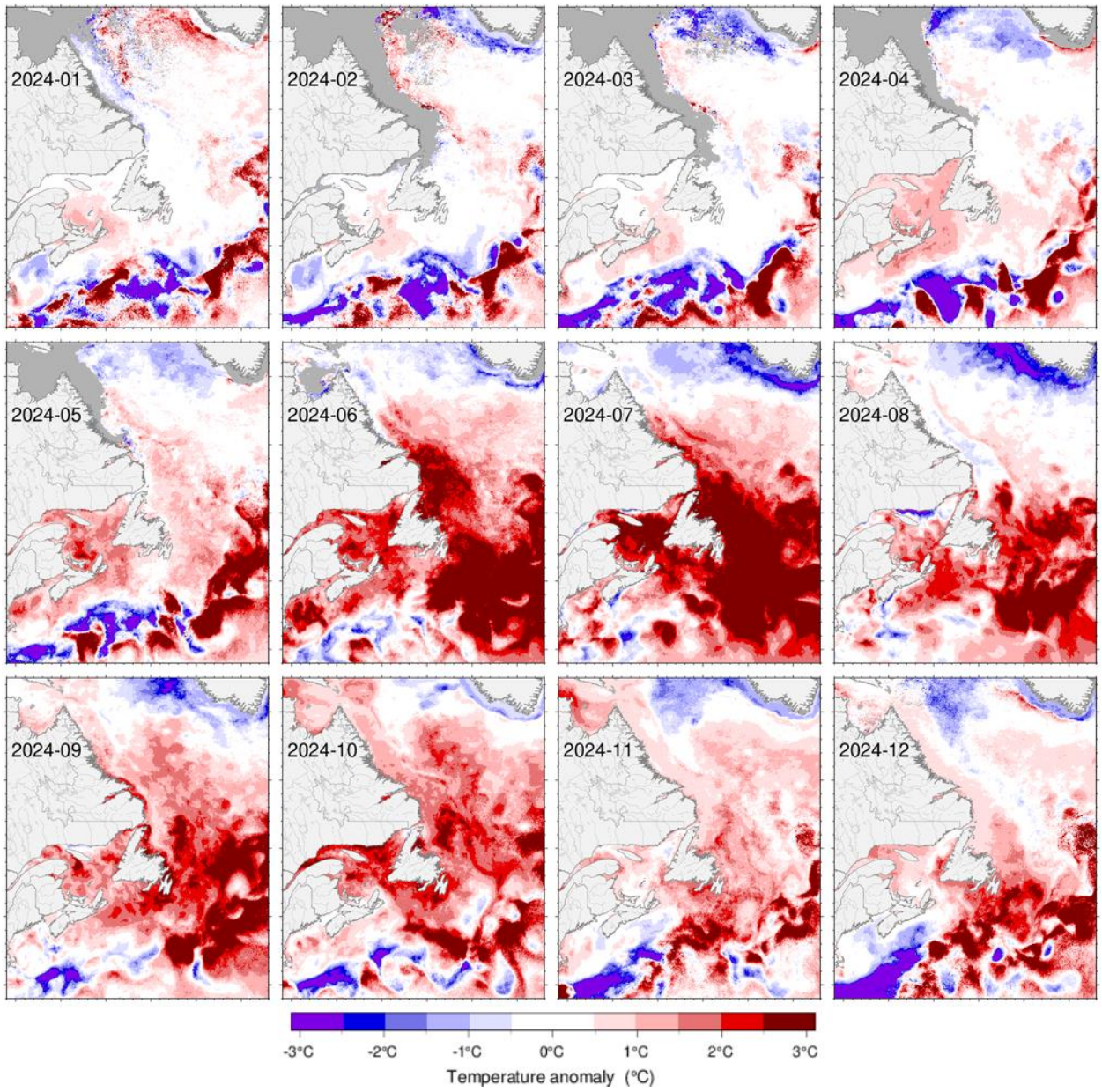

Figure 5. Sea surface temperature monthly anomalies for 2024 in the Atlantic zone based on a 1991–2020 climatology. Areas often covered by sea ice in winter months, such as the Gulf of St. Lawrence, have monthly climatologies that are biased to warm ice-free conditions. Anomalies are not reliable in such areas and months.

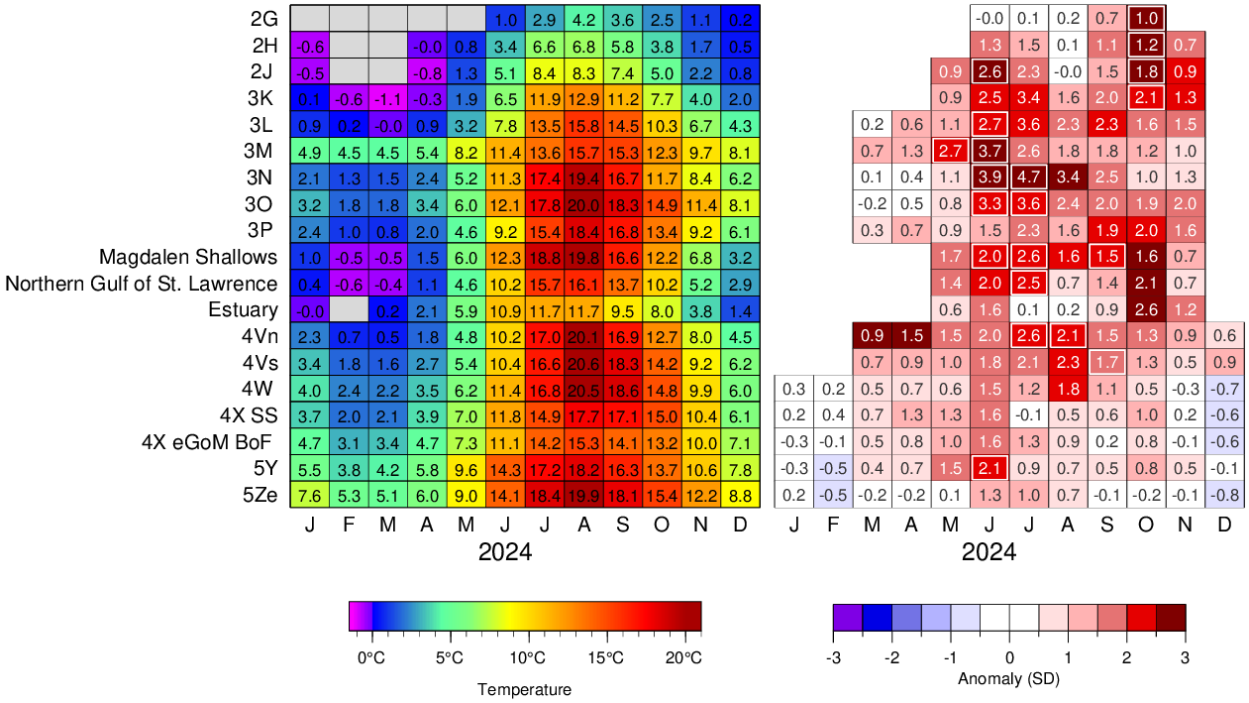

Figure 6. Monthly sea surface temperatures (left) and anomalies in °C (right) for 2024, averaged over the 19 regions shown in the top panel of Figure 2. Regions and months for which the average temperature was at a record high or low are indicated by white outlines. Grey squares have insufficient data coverage to yield a monthly average anomaly (<7%) due to ice cover and clouds. Anomalies are only shown for months having a reliable climatology. Anomalies on the right panel are colour-coded according to the monthly normalized anomalies based on the 1991–2020 climatologies for each month.

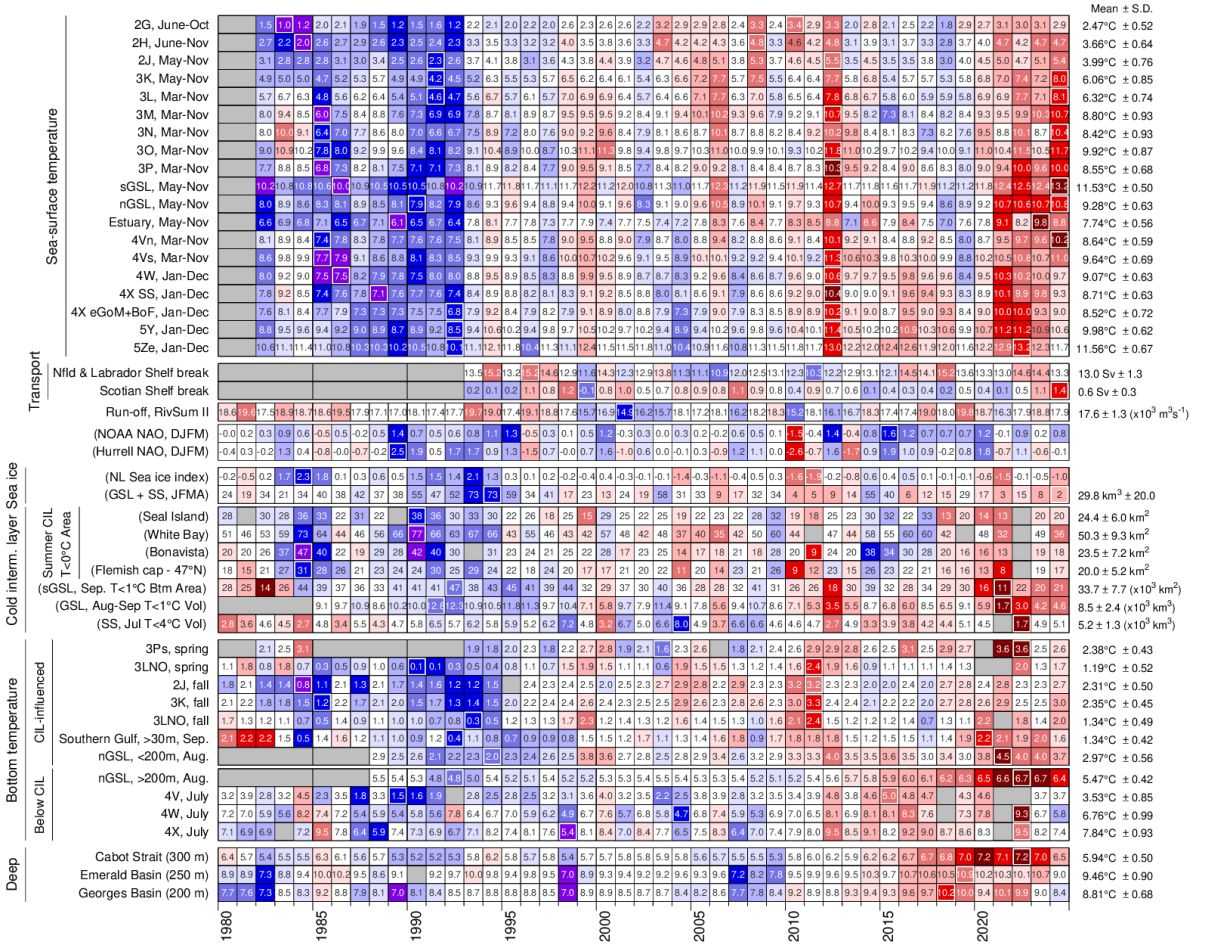

Figure 7. Time series of oceanographic variables, 1980–2024. A grey cell indicates missing data, a white cell is a value within 0.5 SD of the long-term mean based on data from 1991 to 2020 when possible; a red cell indicates above normal conditions, and a blue cell below normal. Variables whose names appear in parentheses have reversed colour coding, whereby reds are lower than normal values that correspond to warm conditions. More intense colours indicate larger anomalies. Series minimums and maximums are indicated by a white outline when they occur in the displayed time span. Long-term means and standard deviations are shown on the right-hand side of the figure. (RIVSUM II is the combined runoff flowing into the St. Lawrence Estuary. North Atlantic Oscillation [NAO], GSL [Gulf of St. Lawrence], SS [Scotian Shelf], sGSL [southern Gulf of St. Lawrence], nGSL [northern Gulf of St. Lawrence], cold intermediate layer [CIL]).

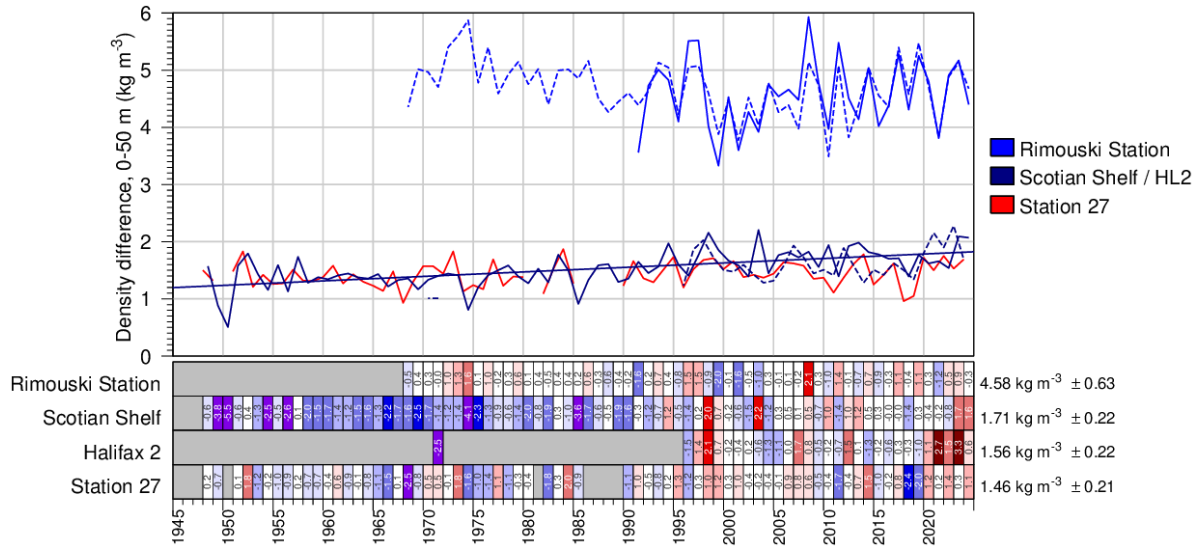

Figure 8. Stratification in the St. Lawrence Estuary (May—Oct average at Rimouski Station), on the southern Newfoundland-Labrador Shelf (May-Nov average at Station 27), and on the Scotian Shelf (shelf average and at Halifax 2 station) The dashed line for Rimouski Station is a proxy based on May—October RIVSUM II freshwater runoff. The solid dark blue line is for the Scotian Shelf average and the dashed line is for the Halifax 2 station. The four bottom scorecard rows show normalized anomalies based on the 1991–2020 period. A grey cell indicates missing data, a white cell is a value within 0.5 SD of the long-term mean, a red cell indicates above normal conditions, and a blue cell below normal.

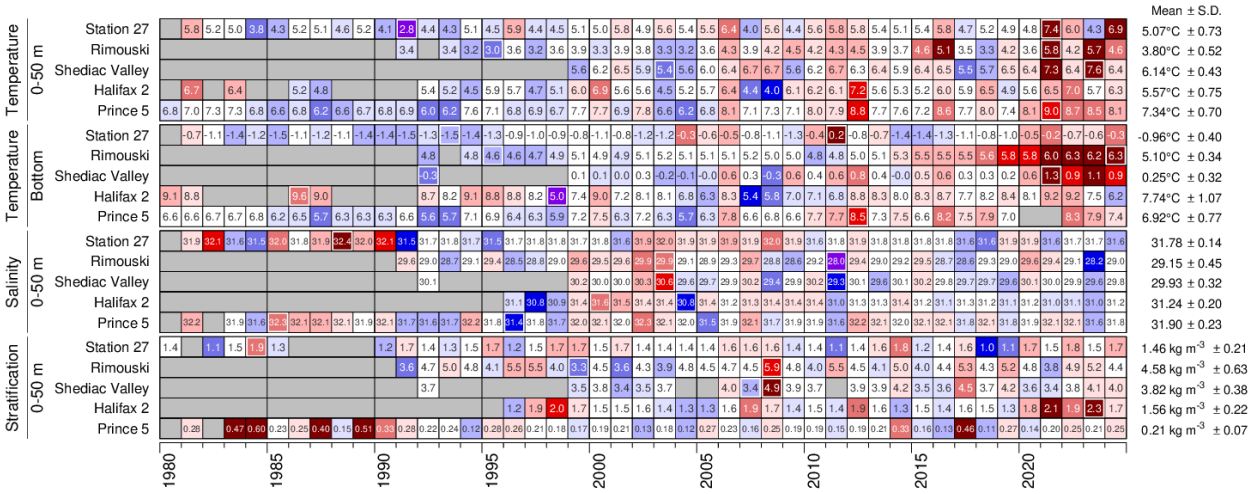

Figure 9. Time series of oceanographic variables at AZMP high-frequency sampling stations, 1980–2024. Values are annual averages at Halifax 2 and Prince 5, May—November at Station 27 and May-October at Rimouski station. A grey cell indicates missing data, a white cell is a value within 0.5 SD of the long-term mean based on data from 1991 to 2020 when possible; for high-frequency station depth-averaged temperature, a red cell indicates warmer than normal conditions, a blue cell colder than normal. More intense colours indicate larger anomalies. For salinity and stratification, red corresponds to above normal conditions. Series minimums and maximums are indicated by a white outline when they occur in the displayed time span. Climatological means and standard deviations are shown on the right-hand side of the figure. Palette as in Figures 6 and 7.

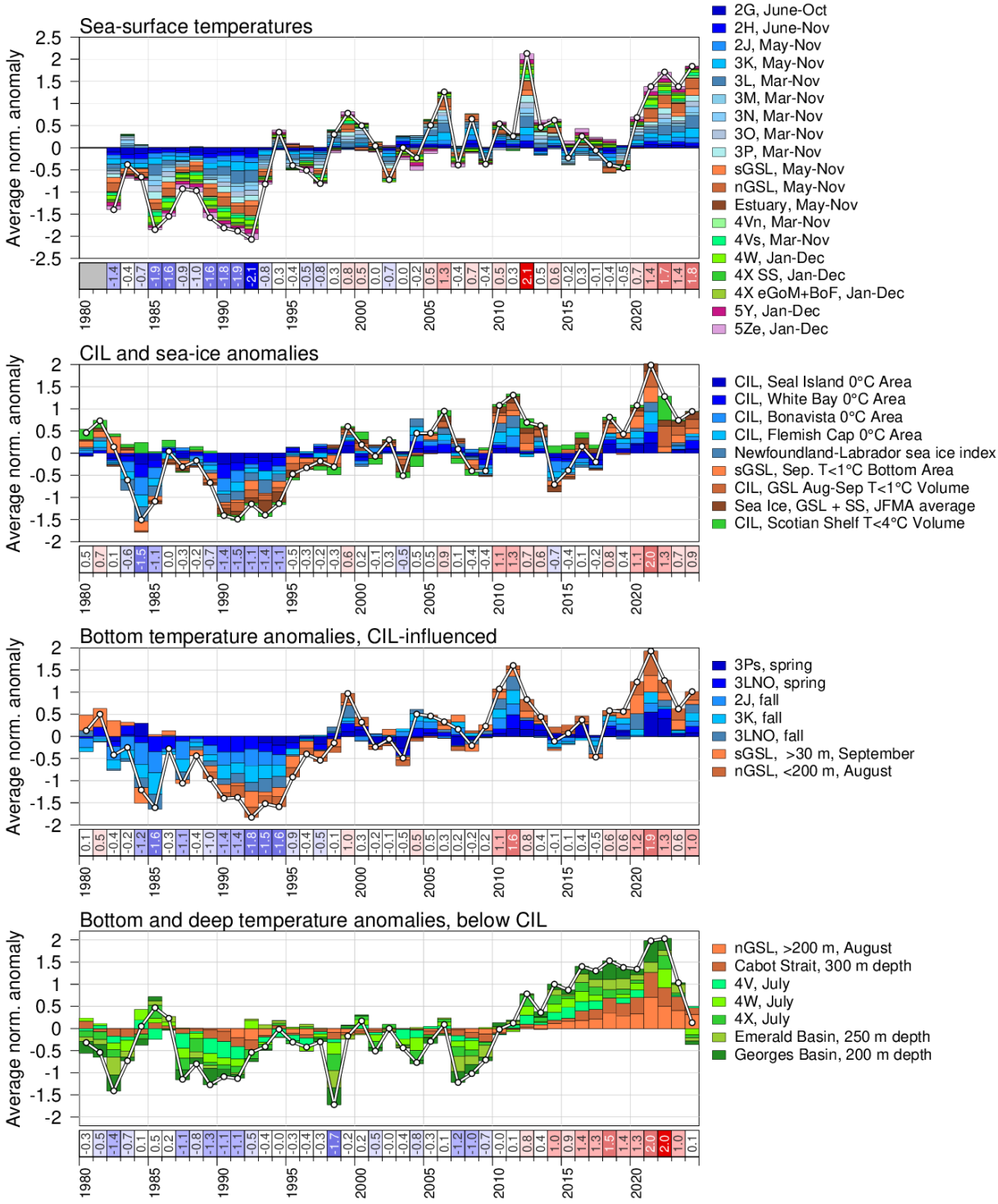

Figure 10. Composite climate indices (white lines and dots) derived by averaging various normalized anomalies from different parts of the environment (coloured boxes stacked above the abscissa are positive anomalies and below are negative). Top panel shows average sea surface temperature anomalies weighted by area, second panel averages cold intermediate layer and sea ice anomalies with areas and volumes in reversed scale (positive anomalies are warm conditions) and bottom panels average bottom temperature anomalies for cold, CIL-influenced waters and for warmer waters found below the CIL.

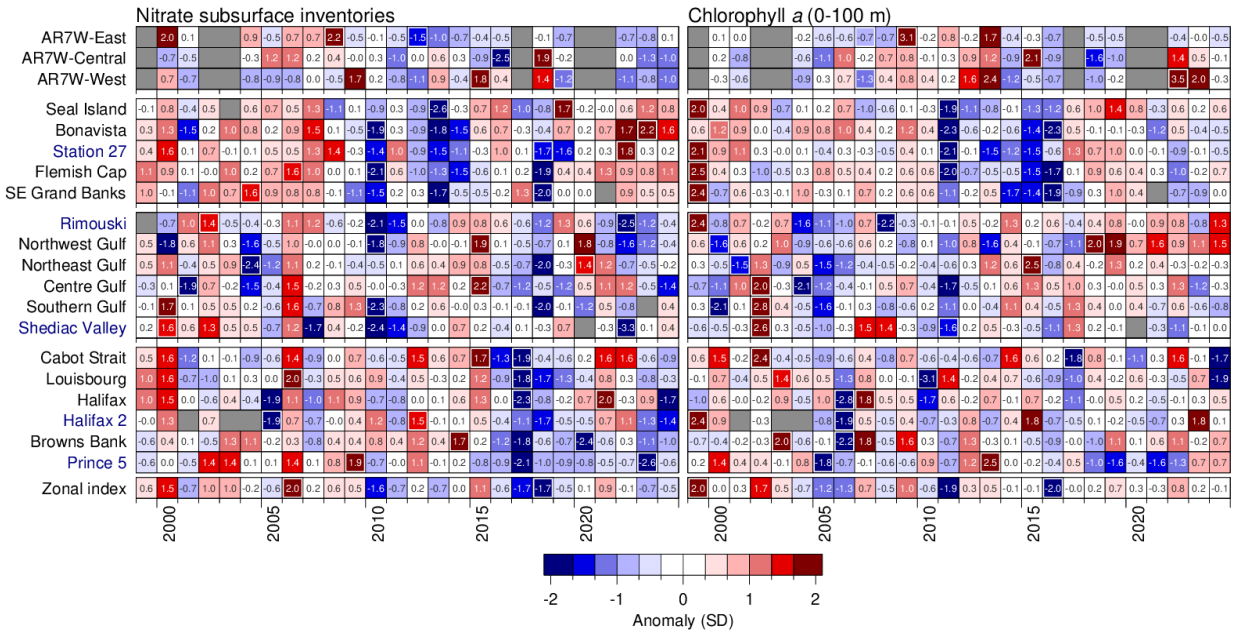

Figure 11. Time series of the subsurface nitrate inventories (100 m — bottom in Labrador Sea; 50–150 m in other regions) and phytoplankton biomass (expressed as chlorophyll *a* 0–100 m inventory) in the Labrador Sea, at AZMP sections, in the Gulf of St. Lawrence averaging areas, and at high-frequency sampling stations (labelled in blue), 1999–2024. A grey cell indicates missing data. A white cell is a value within ⅓SD of the long-term mean based on data from 1999–2020; a red cell indicates above normal inventories, a blue cell below normal. Darker shades indicate larger anomalies; anomaly values are indicated in each cell. Series minimums and maximums are framed in white. The “zonal index” is created as the average of all normalized anomalies, and that result is again normalized. See Figure 1 for the location of sections, averaging areas and stations.

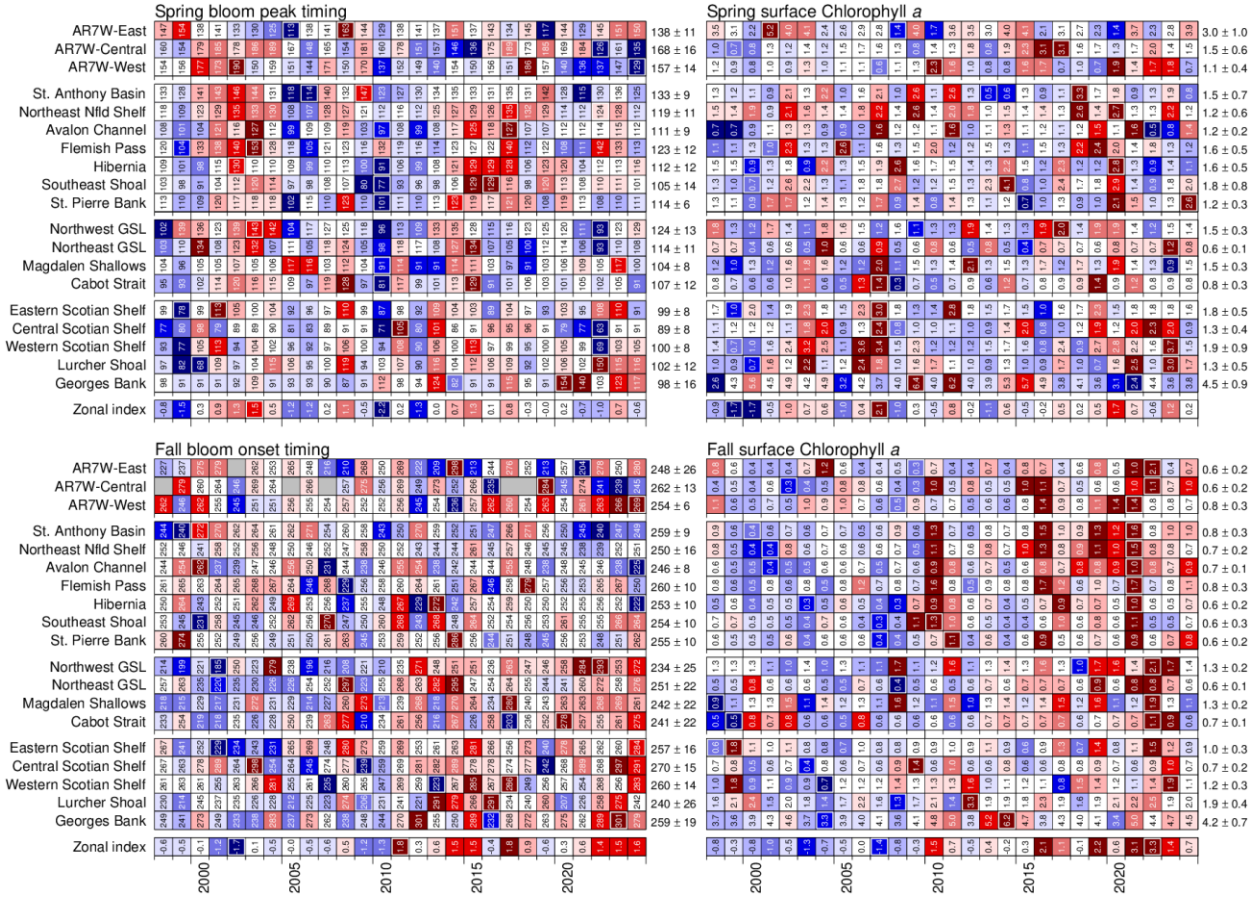

Figure 12. Time series of bloom parameter anomalies derived from remotely sensed surface chlorophyll *a* measurements (spring bloom peak timing, spring chlorophyll *a*, fall bloom onset timing, fall chlorophyll *a*), 1998–2024. Seasonal anomalies are calculated from the daily surface chlorophyll *a* concentration averaged over spring and fall. Data are from OC-CCI (https://www.oceancolour.org/). A grey cell indicates missing data, a white cell is a value within ⅓SD of the long-term mean based on data from 1999 to 2020; a red cell indicates late timing, or above normal inventories, and a blue cell early timing/below normal. Darker shades indicate larger anomalies. Values in cells are days of the year for bloom timing indices and surface chlorophyll *a* concentration (mg m^{-3}) for seasonal averages. White-framed cells indicate series minima and maxima. The "zonal index" is created as the average of all normalized anomalies, and that result is again normalized. See Figure 2 for ocean colour subregion definitions.

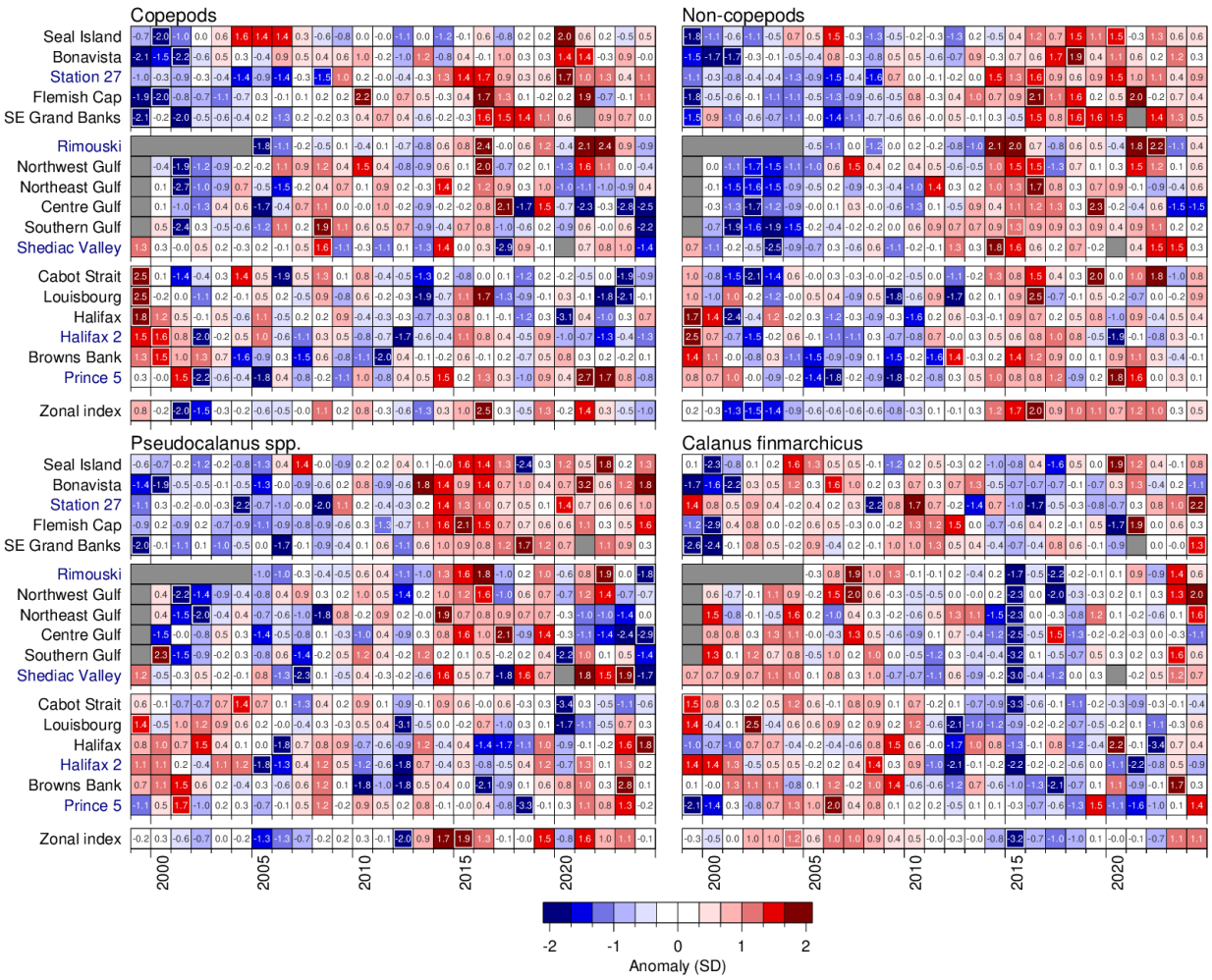

Figure 13. Time series of the abundance anomalies for total copepods, Calanus finmarchicus, Pseudocalanus spp., and non-copepod zooplankton at AZMP sections, in the Gulf averaging areas and at high-frequency sampling stations (labelled in blue), 1999–2024. A grey cell indicates missing data, a white cell is a value within ⅓SD of the long-term mean based on data from 1999 to 2020; a red cell indicates above normal inventories, a blue cell below normal. Darker shades indicate larger anomalies. White-framed cells indicate series minima and maxima. The “zonal index” is created as the average of all normalized anomalies, and that result is again normalized. See Figure 1 for section, averaging areas and station positions.

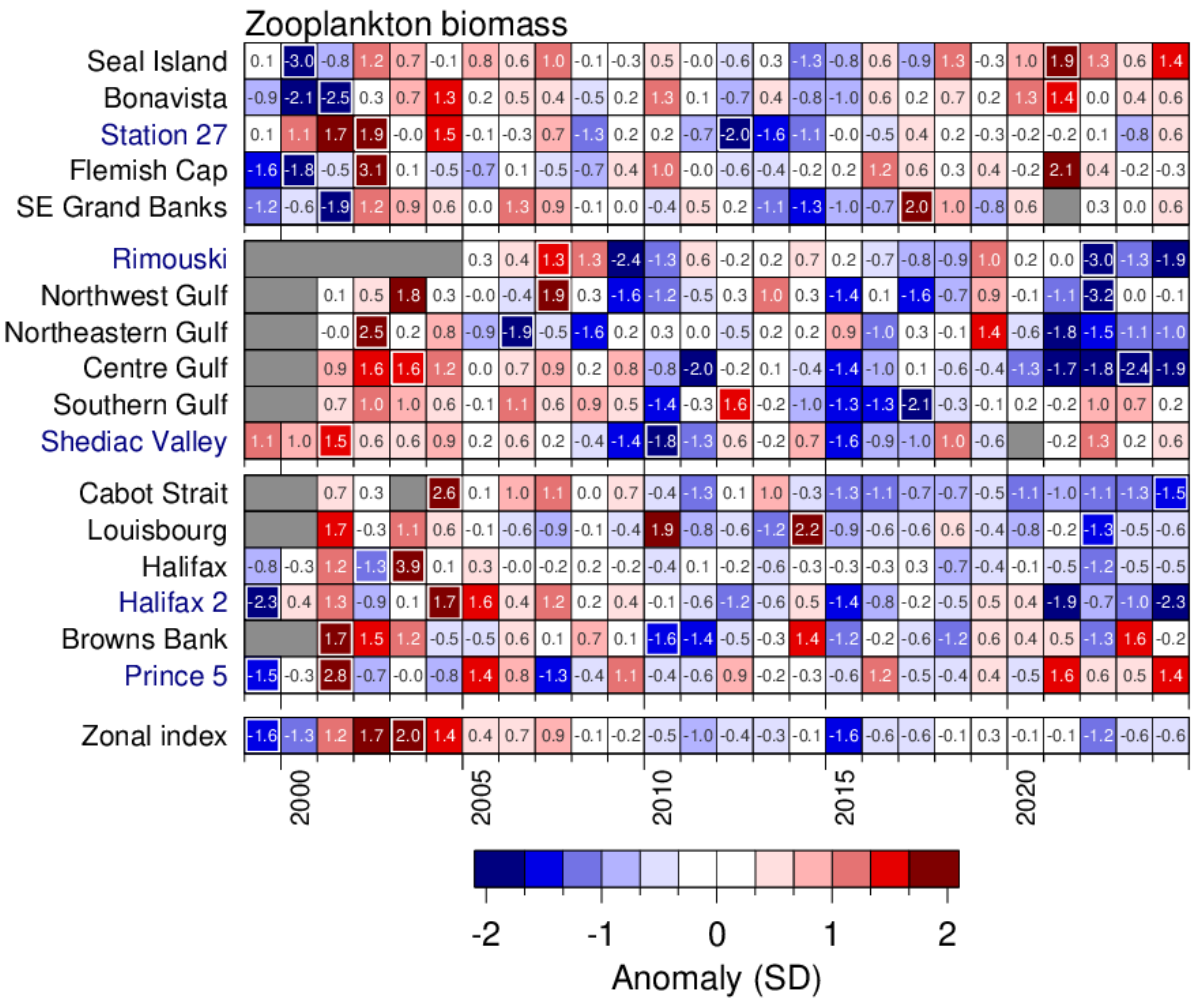

Figure 14. Time series of mesozooplankton dry biomass anomalies at AZMP sections, in the Gulf averaging areas and at high-frequency sampling stations (labelled in blue), 1999 to 2024. Biomass is measured on the 0.2–10 mm size fraction which is usually dominated by copepods. A grey cell indicates missing data, a white cell is a value within ⅓ SD of the long-term mean based on data from 1999 to 2020; a red cell indicates above normal inventories, a blue cell below normal. Darker shades indicate larger anomalies. White-framed cells indicate series minima and maxima. The “zonal index” is created as the average of all normalized anomalies, and that result is again normalized. See Figure 1 for section, averaging areas and station positions.

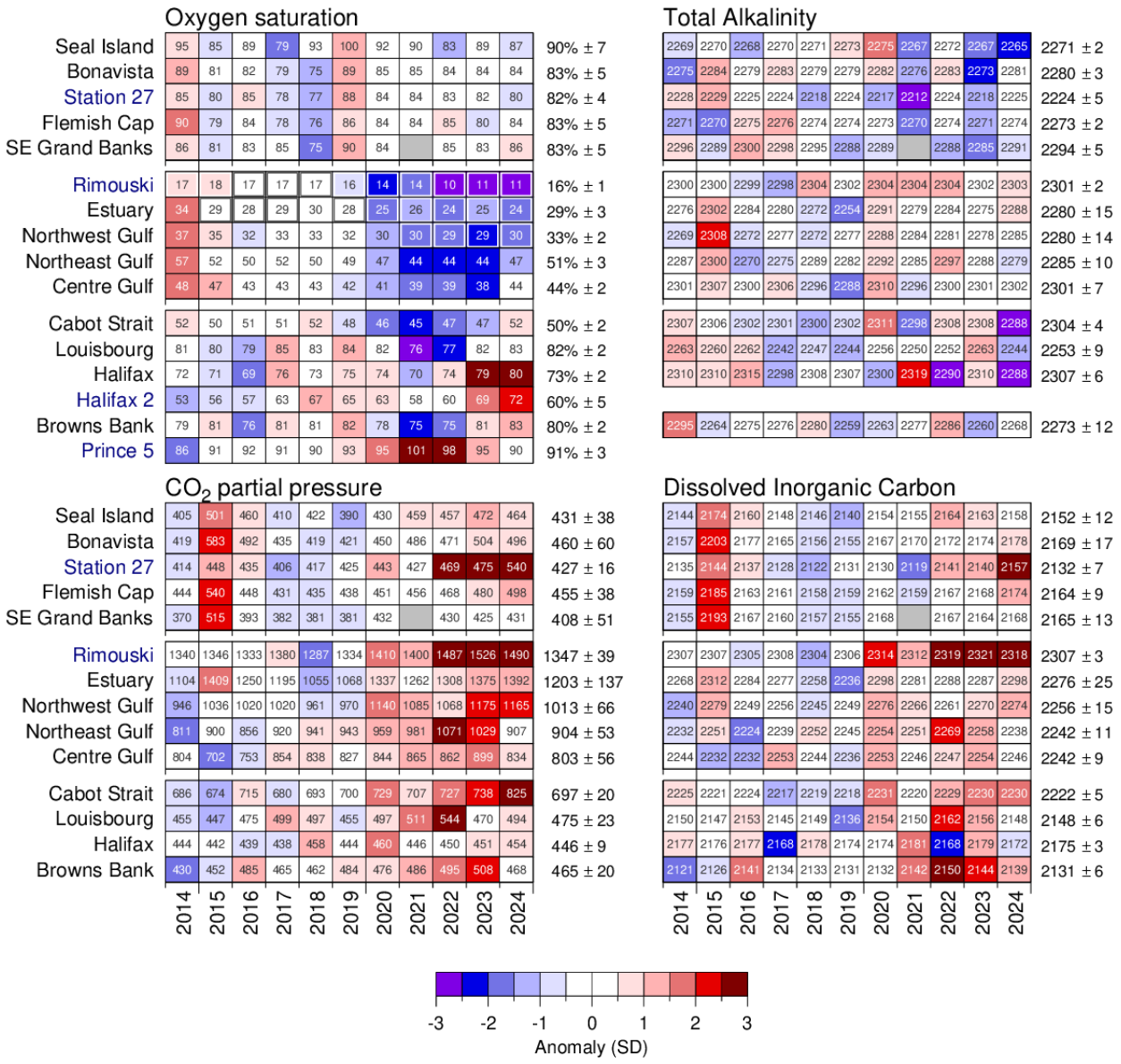

Figure 15. Time series of near-bottom water annual averages for: oxygen saturation (in %, upper left panel); total alkalinity (TA in µmol kg^{-1}, upper right panel); partial pressure of CO_2 (pCO_2 in µatm, lower left panel); and dissolved inorganic carbon (DIC in µmol kg^{-1}, lower right panel) at stations > 100 m in depth, in the Newfoundland and Labrador and Maritimes regions at AZMP sections, in the Gulf of St. Lawrence region averaging areas, and at high-frequency sampling stations (labelled in blue), from 2014 to 2024. A grey cell indicates missing data; a white cell is a value within 0.5 SD of the climatological mean based on data from 2014 to 2020 inclusively; a red cell indicates above normal values; a blue cell indicates below normal values. More intense colours indicate larger anomalies. Climatological means and standard deviations are shown on the right side of each panel. Boxes with borders (either dark grey or white) in the oxygen saturation panel correspond to values at or below the 30% saturation threshold. Near-bottom values represent the deepest observations. See Figure 1 for section, averaging area and station positions.

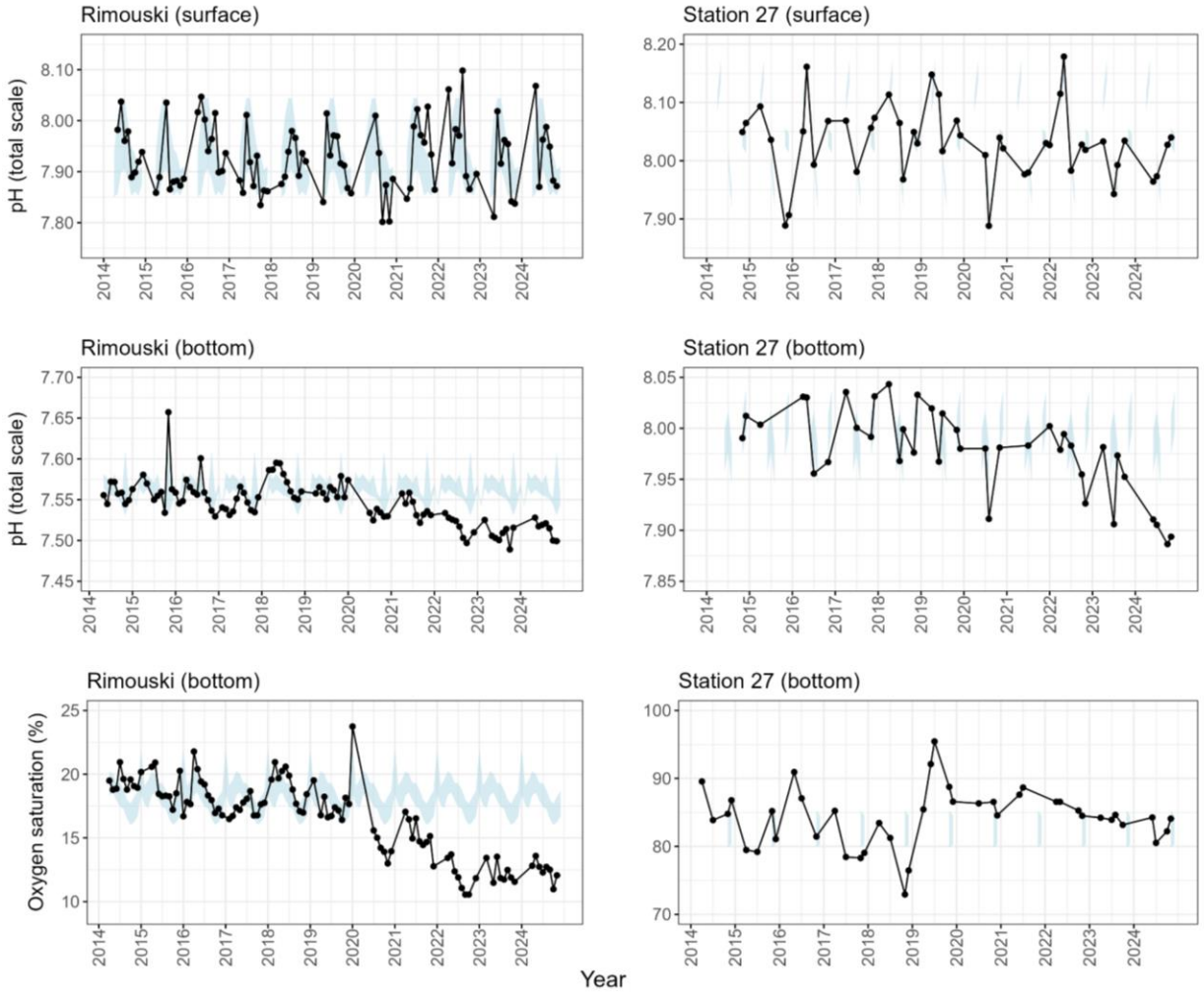

Figure 16. Time series of: (top panels) the monthly average *in situ* pH_T (pH on the total scale) in the surface waters (averaged within the top 15 m) at Station Rimouski in the Gulf of St. Lawrence region (left) and at Station 27 in the Newfoundland and Labrador region (right); (middle panels) the monthly average *in situ* pH_T (pH on the total scale) in the bottom waters at Station Rimouski in the Gulf of St. Lawrence region (left, averaged between 270–320 m) and at Station 27 in the Newfoundland and Labrador region (right, averaged between 150–170 m); (bottom panels) the monthly average dissolved oxygen saturation (%) in the bottom waters at Station Rimouski in the Gulf of St. Lawrence region (left, averaged between 270–320 m) and at Station 27 in the Newfoundland and Labrador region (right, averaged between 150–170 m for pH_T and between 120–170 m for oxygen saturation). The shaded area in blue in each panel indicates the respective monthly climatology for the 2014–2020 period. The relatively short time frame of the climatology, along with occasionally sparse data, may contribute to its noisier appearance. Note the different ranges in scales for pH_T and oxygen saturation in the different panels.

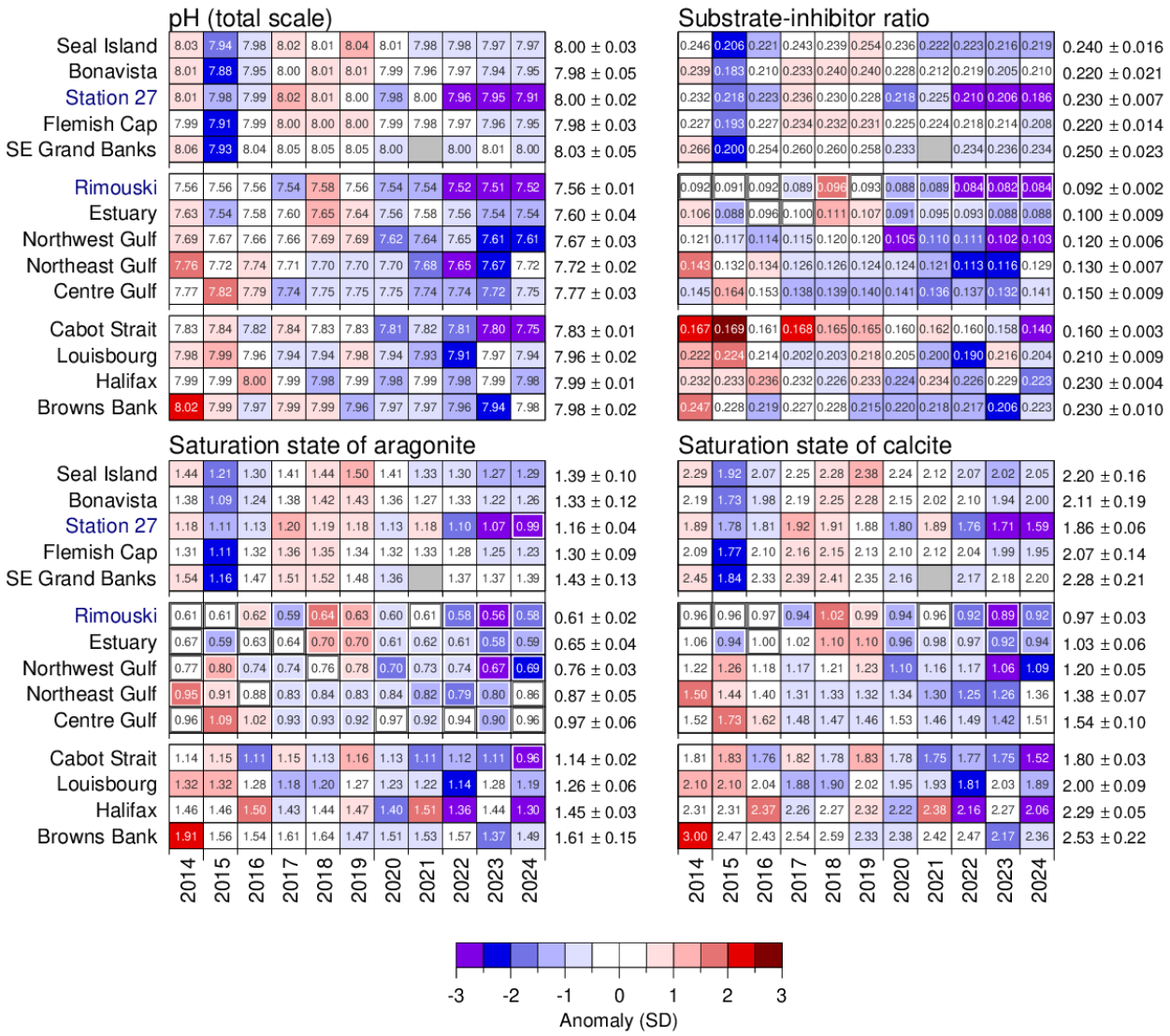

Figure 17. Time series of near-bottom water annual averages for: *in situ* pH_T (pH on the total scale, upper left panel); substrate-inhibitor ratio (SIR in mol µmol^{-1}, upper right panel); saturation state of aragonite (Ω_A—unitless, lower left panel); and saturation state of calcite (Ω_C—unitless, lower right panel) at stations > 100 m in depth, at AZMP sections in the Newfoundland and Labrador and Maritimes regions , in the Gulf of St. Lawrence region averaging areas, and at high-frequency sampling stations (labelled in blue), from 2014 to 2024. A grey cell indicates missing data; a white cell is a value within 0.5 SD of the climatological mean based on data from 2014 to 2020 inclusively; a red cell indicates above normal values; a blue cell indicates below normal values. More intense colours indicate larger anomalies. Climatological means and standard deviations are shown on the right side of each panel. Boxes with borders (either dark grey or white) in the substrate-inhibitor ratio, saturation state of aragonite and saturation state of calcite panels correspond to values at or below the thresholds of 0.1, 1 and 1, respectively. Near-bottom values represent the deepest observations. See Figure 1 for sections, averaging areas and station positions.